Tropical and Extratropical-Origin Storm Wave Types and Their Influence on the East Australian Longshore Sand Transport System Under a Changing Climate

Ian D. Goodwin[1 *], Thomas R. Mortlock[1,2], and Stuart Browning[1]

[1] Marine Climate Risk Group, Department of Environmental Sciences, Macquarie University, North Ryde, NSW 2109, Australia.

[2] Risk Frontiers, Macquarie University, North Ryde, NSW 2109, Australia

[*] Corresponding author. Postal Address: Dept. of Environmental Sciences, Level 2 AHH Building, Macquarie University, North Ryde, NSW, Australia, 2109, Phone: +61 (02) 9850 8354, Email: ian.goodwin@mq.edu.au

KEY POINTS

- Tropical (extratropical) storms produce normal (oblique) propagation of storm waves on shelf
- Tropical expansion impacts coastal stability by reducing headland longshore sand bypassing events
- A significant reduction in northward longshore sand transport in Eastern Australia is projected

ABSTRACT

Tropical expansion is potentially an amplifier of coastal change in the subtropics, through directional wave climate shifts. The storm wave climate and directional wave power distribution along the Southeast Australian Shelf (SEAS) is investigated with respect to tropical extent. Forty years of storm wave observations from nine mid-shelf wave buoys are evaluated using synoptic storm wave typing. A robust latitudinal and along-shelf gradient in storm wave types and wave propagation patterns exists. The tropical origin storms produce a shore-normal propagation pattern along the SEAS, reduce the connectivity of coastal compartments through minor headland bypassing events or episodically reversing the net northward transport. In contrast, the extratropical origin storms produce a shore-oblique propagation pattern from the Southern Tasman to the Coral Sea, and are an important control on the connectivity of regional longshore sand transport through episodic major headland bypassing events between compartments, and the maintenance of down-drift coastlines in dynamic equilibrium. Future climate change projections indicate that the recent trend in the expansion of the latitudinal extent of the tropics in the south-west Pacific region will continue throughout this century. The combined impacts of a projected 2.5° poleward shift on the storm wave climate is a significant reduction in net northward longshore sand transport and the efficiency of headland bypassing events. On the North and Central Coasts of New South Wales we project a ~30% reduction in longshore sand transport for the dominant extratropical-origin storm events, together with a ~5% increase in reversed (net southward) longshore sand transport for tropical-origin storm events.

INDEX TERMS

4217 Coastal processes, 4546 Nearshore processes, 4558 Sediment transport, 4560 Surface

waves and tides, 9330 Australia

KEYWORDS

Storm wave climate, synoptic typing, Southeast Australia, longshore sand transport

1. INTRODUCTION

Extreme storm waves are an important driver of coastal stability, particularly in relation to their magnitude and clustering frequency impacts on coastal erosion, offshore sand transport and subsequent recovery time scales. The directional storm wave climate is also a principal driver of headland bypassing processes through; (i) the establishment of an oblique wave driven current in the littoral zone and the associated longshore sediment transport between obliquely-aligned open coastal compartments; and, (ii) headland-attached rip current leakage of sediment between compartments that are normally aligned to the modal wave climate (Goodwin et al, 2013). Hence, changes in both the extreme values and direction of future storm wave climate have the potential to be major drivers in large-scale coastal reorganisation.

Trend analysis has shown that storm wave heights have been increasing in the North Pacific (Komar and Allan, 2008; Ruggierio *et al*., 2010; Bromirski *et al*., 2013), North Atlantic (Wang *et al*., 2012; Bertin *et al*., 2013, Bromirski and Cayan, 2015), and the Southern Ocean (Young, 1999; Hemer, 2010) in association with a shift towards strengthening extratropical wind fields (Cai *et al*., 2005; Thompson and Solomon, 2002). Whilst there is increasing attention towards the projection of future storm wave climates and extreme values globally under a changing climate (Ruggiero *et al*., 2010; Hemer *et al*., 2013; Dowdy *et al*., 2014), a

major unknown is whether the poleward expanding tropics (the width of the Hadley Cell) (Seidel *et al*., 2008) will be associated with a shift in the relative frequency and magnitude of tropical or extratropical storm waves, and a corresponding shift in directional wave climate.

The modal wave climate along the Southeast Australian Shelf (SEAS) is dominated by waves from south to east-south-east. South of 33°S, this directional wave climate is quasi-normal to the shelf and coast, whereas north of 33°S, the wave climate becomes increasingly oblique to the shelf and coast strike. This drives a northward longshore current and sand transport over ~1000 km from the central NSW coast as far north as 28° S, (shelf north of Fraser Island,) with transport rates increasing from ~50,000 m^3/yr to ~1,000,000 m^3/yr (Boyd *et al.*, 2008). The East Australian longshore sand transport system is one of the largest longshore sand transport systems on Earth and connects regional coastal compartments via major headland bypassing (Figure 1). The late Quaternary evolution of the great sand islands, such as Stradbroke Is., Moreton Is., and Fraser Is. in south-east Queensland is manifest to this longshore transport system.

In the south-west Pacific region, extreme waves are generated from either: (i) poleward-moving tropical cyclones in the Coral Sea; (ii) in the Tasman Sea from East Coast Lows of both subtropical and extratropical origin; and, (iii) in the Southern Tasman Sea by extratropical lows cut-off from the circumpolar trough (Browning and Goodwin, 2013). Hence, the broad-scale synoptic drivers are strongly linked to latitudinal interactions of subtropical and extratropical air masses. These storm systems generate south to east extreme waves from Southern Tasman Sea sources, and east through north-east extreme waves from the northern Tasman Sea to Coral Sea sources (Goodwin, 2005). Typically, the mid-shelf environment (SEAS) experiences a maximum (hourly) peak storm significant wave height of between H_s = 7.1 m (Eden) and 8.9 m (Sydney), and mean peak storm significant wave height of H_s = 3.7 to 4.0 m, with mean storm durations of 60 to 90 hours (Shand *et al.*, 2011).

92 Previous studies on projecting storm wave frequency and magnitude for climate-change
93 scenarios later this century group all storm wave events into either Tropical Cyclones or East
94 Coast Lows and focus on coastal impacts of changing storm frequency (e.g. Hemer *et al*.,
95 2013; Dowdy *et al.*, 2014). The recent Tropical Expansion trend is most apparent during the
96 equinoxes, which is of significance for the understanding of storm wave event time series,
97 because of the warm season (late summer -autumn) occurrence of high magnitude East Coast
98 Lows along the north coast New South Wales (NSW). Tropical expansion is projected to
99 continue over the future century and since our *a priori* observations show contrasting
100 directional storm waves for either tropical or extratropical origin, we investigate the
101 latitudinal relationship of the storm wave types and the impact of future tropical expansion
102 and potentially more tropical-origin storms on the East Australian longshore sand transport
103 system.

104 The paper is divided into four components: (i) a synoptic typology of storm wave events
105 along the SEAS, their latitudinal relationship and deepwater propagation patterns; (ii)
106 nearshore directional wave power patterns for characteristic coastal compartments; (iii) the
107 contribution of each storm wave type to potential longshore sand transport; and (iv) the
108 implications of a changing storm wave climate on headland sand bypassing and the
109 connectivity of regional longshore sand transport.

110

111 ## 2. DATA AND METHODS

112 ### 2.1 Instrumental Extreme Wave Data

113 Along the SEAS, instrumental wave data have been collected since the mid 1970s when the
114 New South Wales (NSW) and Queensland (QLD) Governments commenced wave

115 monitoring. Long-term, continuous and directional wave data are available for mid-shelf
116 locations at (north to south) Byron Bay, Coffs Harbour, Crowdy Head, Sydney, Port Kembla,
117 Batemans Bay and Eden (Figure 1). In addition, Sydney Ports Corporation has maintained a
118 wave buoy offshore of Botany Bay since 1971. Further north, the Queensland Department of
119 Science, Information Technology, Innovation and the Arts (DSITIA) maintains a network of
120 12 wave buoys along the QLD coastline. A wave buoy located offshore of Brisbane (Point
121 Lookout on North Stradbroke Island) since 1976 improves the evaluation of subtropical wave
122 climate in far north NSW, and is used in this study. Table 1 shows the length of directional
123 and non-directional wave observations for each buoy used in this study (after Kulmar *et al*.,
124 2013). This dataset provides observational coverage of approximately 1,000 km of mid-shelf
125 waves (60 – 100 m depth), along the western boundary of the Tasman and Coral Seas from
126 27 to 37° S. Although most modal wave conditions are likely to be deep-water waves at the
127 buoy locations (where water depth is greater than half the wavelength, $d > L/2$), this condition
128 is not always satisfied for storm waves travelling at periods of 10 s or more. This study
129 therefore deals with a mid-shelf, intermediate-to-deepwater storm wave climatology.

130 All buoys measure hourly wave spectra, from which parametric data is derived. In this paper
131 we use the 1-hourly significant wave height, H_s (m), wave period at the primary spectral
132 peak, T_p (s), and mean wave direction, *MWD* (degrees True North, ° TN), to describe storm
133 wave characteristics.

134 2.2 Extreme Value Analysis

135 An extreme value analysis of this instrumental wave data archive (start of record to
136 December, 2009) was reported in Shand *et al.* (2011) and the database was made available
137 for our study. A Peak over Threshold (PoT) analysis was undertaken to define storm events
138 (Shand *et al.*, 2011) for 1-hourly significant wave height, H_s, of greater than 2.0 m

(approximate to the 10% exceedance wave height along the NSW/QLD coast) with a minimum exceedance duration of three days. A second higher threshold of 3.0 m (5% exceedance threshold) with no minimum duration was also used to capture intense but transient storms (e.g. tropical cyclones). A minimum interval between storms was set at one day to prevent single storms being split into two or more events if wave height temporarily drops below the threshold. Mortlock and Goodwin (2015) tested the storm event frequency returned using these values and found them to give a statistically robust split between storm and modal wave conditions.

We extend the use of wave buoy observations to 2013 for the analysis of storm wave shoreface refraction patterns in Section 4 and implications for regional longshore sand transport in Section 5. We consider the length of this wave data spanning ~40 years to be appropriate for the study of extreme waves, as it is sampled from both phases of the Interdecadal Pacific Oscillation (IPO) that has been previously shown to influence the SEAS wave climate (Goodwin, 2005).

2.3 Synthesis of Storm Wave Parameters

Average storm-peak parameters H_s, T_p and *MWD* for each storm type were determined using the database of Shand *et al*. (2011) (Table 2). For the Central Coast NSW (extents Figure 1), storm peak H_s and T_p parameters were derived from storm events identified from the Sydney and Port Kembla buoy records (1974 – 2009), and *MWD* from the available (1992 - 2009) directional Sydney record. For the Mid North Coast NSW, storm peak H_s and T_p were derived from storm events identified from the Coffs Harbour buoy record (non-directional 1976 - 2009), and *MWD* was hindcast from the directional portion of the Byron Bay record (2000 - 2009) (method Section 2.3.1). For the North Coast NSW, storm peak parameters were derived from the Byron Bay buoy (non-directional from 1977, directional from 2000), except

for ETLs where the peak storm wave direction was determined from the Brisbane buoy record. This was because observed East Coast Lows are understood to be under-sampled at Byron Bay due to issues of buoy submergence during early deployments (Shand *et al.,* 2011). The number of East Coast Lows recorded at Brisbane and Byron Bay is comparable between sites.

2.3.1 Storm Wave Direction Hindcast

Since the Coffs Harbour buoy only became directional in 2012, no directional information for storm types was available in the original Shand *et al.* (2011) report, which was concluded in 2009. Instead we used the directional portion of the Byron Bay buoy record, 190 km north of Coffs Harbour, to hindcast *MWD* for storms back to 2000 at Coffs Harbour. The Byron Bay buoy is the nearest mid-shelf buoy with an interannual directional record.

We used a cumulative distribution function (CDF) matching approach (Brocca *et al.*, 2011) between the overlapping directional records at Byron Bay and Coffs Harbour (February 2012 – December 2013), giving a training dataset of over 12,000 hourly observations (Figure 2). Only wave directions between 20 and 200° (i.e. onshore-propagating wave energy) were used to train the model. Although *MWD* is broadly comparable between the two sites (Figure 2a), bias-adjustment was found to better describe the *MWD* distribution, especially the peaks around 40 and 150° characteristic of the Coffs Harbour record (Figure 2c). Once *MWD* was hindcast for the non-directional portion of the Coffs Harbour record (back to 2000), the peak-storm *MWD* for each storm type could be determined (Table 2).

2.4 Storm Wave Typology and Relationship to Large Scale Climate

In this study, we have refined the maritime storm typology of PWD (1985, 1986) and Speer *et al.* (2009) according to the Browning and Goodwin (2013) investigation of storm tracks

and meteorological evolution of: (i) the extratropical transition of cyclones from the Coral Sea; (ii) the evolution of subtropical maritime storms over the Tasman Sea; and, (iii) the subtropical transition of extratropical storms cut off over the Southern Tasman Sea. Each storm type is related to tropical extent by the latitude of the zonal maximum mean sea-level pressure MSLP (Subtropical Ridge, STR) in the Tasman and Coral Seas region bounded by 10°-44° S and 145°-150° E (Drosdowsky, 2005). The mean latitude of the STR was calculated using ERA-Interim MSLP data using a modified L-index (Pittock, 1973; Drosdowsky, 2005).

Each PoT storm wave event in the Shand *et al.* (2011) database was assigned to one of the eight synoptic types storm types listed in Table 3. The synoptic type for each wave event was based on the synoptic genesis of the storm, including storm track and the synoptic pattern at the time of the observed peak wave climate using the 1000 hPa (surface) and 500 hPa pressure field data from the NCEP-NCAR Reanalysis (NNR) mean sea-level pressure dataset from 1948 to 2009 (Kalnay *et al.*, 1996).

2.5 Storm Wave Generation and Propagation Patterns

We composited the mean H_s and *MWD* for all recorded storm wave events for each storm type, using the ERA-Interim gridded wave data (1980 to 2011). Previous studies have shown that wave data from the ERA reanalyses (Dee *et al.*, 2011) show positive trends in high percentile wave heights around the southern margin of Australia (Hemer, 2010), and during austral winter and southerly wave conditions in the Tasman Sea (Harley *et al.*, 2010). In order to minimize wave height bias, we used the ERA-interim H_s rather than maximum wave height (H_{max}) values for each storm day to examine relative differences in the propagation patterns for each storm type.

2.6 Modelling Storm Wave Shoreface Refraction Patterns

A MIKE21 Spectral Wave (SW) model was used to transform offshore peak storm wave parameters for the four most frequent storm types (Table 2) to three characteristic coastal compartments: (i) Central Coast NSW (Terrigal-Wamberal Beach, a closed to leaky compartment); Mid North Coast NSW (Sawtell Beach, a leaky to open compartment); and, (iii) North Coast NSW (Byron Bay, an open compartment) (locations Figures 1 and 3). MIKE21 SW is a third-generation, phase-averaged spectral wind-wave model that computes random, short-crested wind-waves in coastal and inland regions (DHI, 2016). In this instance, the model solves the wave action conservation equation using a directional decoupled parametric formulation.

A separate model domain was created for the shelf region that encompassed each of the three study sites. For each location, the wave model domain extended approximately 30 km of shoreline length either side of the study site out to the 70 to 90 m isobaths on which the mid-shelf waverider buoys were moored. This ensured that lateral boundary errors did not propagate into the areas of interest, and that offshore wave forcing represented those observed at the mid-shelf buoys.

A flexible mesh was used, grading from an approximate mean element length of 200 m offshore to 50 m at the shoreline in order to capture bathymetric complexities affecting refraction patterns in shallow water. The seabed topography was described using a mosaic of best-available bathymetries from the depth of offshore buoys to the shoreline. Where no localised bathymetries were available, gaps were filled using the GeoScience Australia AusBathy grid (Whiteway, 2009). A buffering method was used to avoid depth-stepping between adjacent bathymetries.

A JONSWAP spectrum was used to propagate spectral information through the model domain based on boundary parameters of peak storm H_s, T_p and *MWD* for each storm type. A

234 directional spreading function equivalent to approximately 20° of spreading was used to
235 replicate a mixed sea-swell environment characteristic of storm wave conditions.

236 *2.6.1 Model Validation*

237 The model's nearshore performance was validated against observations from two Datawell
238 Directional WaveRider (DWR) buoys deployed at Wamberal and Sawtell (locations Figure
239 3), giving a validation record of over 1,900 hourly observations. During validation, MIKE21
240 SW was run using hourly wave parametric data from the closest offshore wave buoy over the
241 period of nearshore observations (i.e. Sydney buoy for Wamberal, Coffs Harbour buoy for
242 Sawtell, see Figure 3 insets).

243 The model performed well in the prediction of nearshore H_s ($R^2 > 0.90$, slope 0.90) and *MWD*
244 ($R^2 > 0.80$, slope 0.82), but over-predicted wave period by 1-2 s at both sites (Figure 4). The
245 systematic over-prediction of wave period is probably a result of no wind forcing during
246 model validation. A local wind was not applied because the model was used with
247 representative storm wave parameters, for which no corresponding wind field existed.

248 Despite the discrepancy in wave period, the accurate modelling of H_s is the most important
249 parameter for the representation of directional wave power, P, as P is proportional to the
250 square of the wave height (from Holthuijsen, 2007):

251 $$P = EC_g \tag{1}$$

252 where E is the wave energy density, C_g is the wave group velocity (m/s), and P is expressed
253 in kilowatts per meter wave-crest-length (kW/m). To account for shoaling effects, C_g is
254 defined as $n\ \lambda/T_p$ where λ is the wavelength determined using the Newton-Raphson
255 iterative solution and n scales with depth:

256
$$n = \frac{1}{2}\left(1 + \frac{4\pi d/\lambda}{\sinh\left(4\pi d/\lambda\right)}\right) \quad (2)$$

257 2.7 Modelling Potential Longshore Sand Transport at Updrift Headlands for Storm Types

258 The longshore sand transport rate during peak storm wave conditions was determined for the
259 four most commonly-occurring storm types at each of the three study sites. Wave data was
260 output at ~ 5 m water depth off the southern headland at each site to determine the influence
261 of a change in storm type with tropical expansion on headland sand bypassing (output
262 locations Figures 8 - 10). The strike of the 5 m contour was calculated as the best-fitting
263 tangent to the 5 m contour along the updrift coast and headland at each site. This value is an
264 approximation of 'real-world' bathymetry and is a valid method to compare the sand
265 transport rates for each storm type.

266 The potential volumetric transport rate, Q, was calculated using the CERC equation (after
267 Rosati *et al*., 2002);

268
$$Q = K\left(\frac{\rho\sqrt{g}}{16\kappa^{\frac{1}{2}}\left(\rho_s - \rho\right)\left(1-n\right)}\right)H_b^{\frac{5}{2}}\sin\left(2\alpha_b\right) \quad (3)$$

269 where ρ is the density of seawater (1,025 kg/m^3), g is acceleration due to gravity (9.81 m/s^2),
270 H_b is the breaker wave height (here, the storm peak H_s at ~5 m depth), α_b is the wave
271 obliquity at the breaker line, k is the breaking coefficient (set at 0.8), ρ_s is the density of
272 immersed sand (set at 2,650 kg/m^3) and n is the porosity of sand (set at 0.4). The
273 proportionality coefficient, K, was determined using the relationship of del Valle *et al*.
274 (1993);

275
$$K = 1.4e^{(-2.5D_{50})} \quad (4)$$

where D_{50} is the median grain diameter (set at 0.19 mm, after Roy and Stephens (1980), who show outer nearshore deposits are composed of quartz sands of this grain size across the NSW inner shelf). Sediment characteristics were left unchanged at each site to elucidate the impact of storm wave conditions on headland transport.

3. STORM WAVE TYPES AND PROPAGATION PATTERNS

The discrimination of storm wave events into tropical or extratropical origin, and their seasonality, is an important first step in reducing the problem of how storm wave climatology might change in the future, and hence the impact on event-level and net longshore sediment transport. A synoptic description of the eight storm types covered by the terms Tropical Cyclones and the Subtropical East Coast Lows (ECL) is included in Table 3. Tropical origin storm wave events are generated by storms in the Central Tasman Sea to Coral Sea (Easterly Trough Lows (ETL), Inland Trough Lows (ITL), Tropical Cyclones (TC), Tropical Depressions (TL) and Anticyclone Intensification (AI)). Extratropical origin events are generated in the Southern Tasman Sea (Southern Secondary Lows (SSLs), Continental Lows (CL) and Southern Tasman Lows (STL)). The MSLP field associated with each of the eight storm types is shown in Figure 5. The corresponding fetch and ocean wave propagation patterns are shown in Figure 6 a – h (for peak storm wave energy at the buoy locations).

East Coast Lows exhibit strong seasonality in their occurrence. The primary Austral winter events are ETLs (April to August), SSLs (May to October), and STLs that occur primarily between July and December. TCs and TLs are warm season weather systems (December to April with most occurring between January and March). Hybrid tropical-extratropical events such as Inland Trough Lows (ITL) have a larger frequency during October to March. and Anticyclone Intensification (AI) events tend to be more concentrated and produce larger

storm waves between January and June (Shand *et al.,* 2011). ETLs, ITLs, SSLs and STLs are the most common storm types along the SEAS (over 75% of the variability in the storm wave climate), apart from on the North Coast NSW where AIs replace STLs. A full discussion of storm frequency for each region is provided in Shand *et al*., (2011). We examine the impact of the four most common storm types on the nearshore processes in sections 4-6 of the paper.

The latitudinal association of each storm type results in an along-shelf distribution of storm type occurrence along the SEAS (all buoy records, Figure 7a). In general, STLs produce the most southerly storm wave patterns emanating from the Southern Tasman Sea. SSL produce southerly patterns, whilst AI and ITL's produce south-easterly patterns along the coast and shelf south of 30° S. ETLs produce east-south-easterly patterns along the entire coast and shelf from 25 to 40° S. ETLs are the most powerful storm type across the shoreface at all sites, due to the highest mid-shelf wave height and most shore-normal wave direction.

There is also a strong along-shelf gradient in storm wave direction, as shown in the directional record at mid-shelf buoy locations (Brisbane, Byron Bay and Sydney buoys, shown in Figure 7b). Mean storm wave direction is 129 ° at Brisbane 147 ° at Byron Bay and 153 ° at Sydney, thus rotating clockwise with latitude south. While a significant SE component is visible at all three buoys, Sydney receives the largest storm waves from the SSE and Brisbane from the ENE, reflecting the proximity to different storm wave genesis (i.e. from Figure 7a, storm wave genesis of AIs, TCs and ETLs is most proximal at Brisbane, and STLs and SSLs are most proximal at Sydney).

4. REGIONAL SHOREFACE EXPOSURE TO STORM WAVE TYPES

Nearshore sensitivity to variability in storm wave types is shown in Figures 8-10 for each storm type at Terrigal-Wamberal (Central Coast NSW), Sawtell (Mid North Coast NSW) and

Byron Bay (North Coast NSW) when offshore peak-storm wave parameters (given in Table 2) were refracted across the shelf. The difference in wave power refraction patterns between sites is due to: (i) the south-to-north latitudinal wave power gradient; and, (ii) the shoreface slope and aspect at each location (Figure 3). The mean upper (lower) shoreface slope and aspect at Wamberal is approximately 2.2% (1.4%) and SE, at Sawtell and Byron Bay is 1.9% (0.6%) and ESE and NE, respectively. The shoreface slope at each site was determined by taking a shore-normal transect through the bathymetric surface used for wave modelling. Each transect extended from the centre of each study site from the shoreline to 30 m depth. The slope of the upper shoreface was defined as the shore-normal gradient from the shoreline to 12 m depth (15 m at Wamberal), and from 12/15 m to 30 m depth for the lower shoreface. The compartment aspect was defined as the shore-normal direction from the centre of each study site.

A steeper, narrower shoreface, and planform orientation towards the mean storm wave direction at Wamberal (and Central Coast NSW in general), combined with the proximity to southerly storm wave generation, increases the exposure to high nearshore storm wave power towards the more exposed northern end of the embayment. At Sawtell (and on the Mid North Coast in general), a more easterly shoreline geometry means there is particularly high (> 90 kW/m) exposure to ETL storm wave events.

A lower nearshore wave power environment exists at Byron Bay (and on the North Coast in general) because of the increased distance from southerly storm wave generation (for SSL, ITL and STLs) and exposure to less intense storm type (for AIs). Locally, the pattern of nearshore wave power at Byron Bay is also influenced by refraction around Cape Byron, Julian Rocks and a prominent shelf sand-body east of Cape Byron (see Goodwin *et al*, 2013). These features further dissipate wave energy producing much lower nearshore wave power environment.

In summary, the largest along-shelf contrast in storm wave direction is between the STL/SSL and ETL storm wave climates that range from strongly oblique to normal to the shelf strike direction, respectively (Figure 11a). After refraction across the inner shelf and shoreface, the directional difference between the SSL and ETL storm waves increases with decreasing latitude (i.e. northward).

5. INFLUENCE OF STORM TYPES ON PRESENT AND FUTURE REGIONAL LONGSHORE SAND TRANSPORT

5.1 Potential Longshore Sand Transport Rates Associated with Storm Type

The present-day oblique SE mean wave climate leads to an increasing net differential in the longshore wave-driven current to the north along the SEAS. Superimposed on this, storm-wave events facilitate episodic headland sand-bypassing to downdrift headland-bay beaches, or offshore transport to the lower shoreface. Headland bypassing of sand between coastal compartments is facilitated by shoreline planform accommodation space through the clockwise rotation of the surf zone bar system under modal wave conditions, and is episodically driven by obliquely propagating storm wave energy (Goodwin *et al.*, 2013). The directional wave climate thus performs the role of a 'sand valve' updrift of each headland.

To quantify the influence of each storm type on headland sand bypassing we modeled the potential longshore sand transport rate, updrift of the major headlands using the wave obliquity and wave height output during the storm peak, at the ~5 m depth contour off the updrift headland at each of the three study sites (locations Figures 8 to 10). The results of the calculated storm-peak potential longshore sand transport, Q (m^3/hr), for a typical storm event, are listed in Table 4.

372 At all sites ITLs and SSLs produce an equivalent potential sand transport rate. At Terrigal-
373 Wamberal a typical ETL drives a net northward potential sand transport rate of ~8,400 m^3/hr,
374 which is 30% greater than that of a typical SSL, although SSLs are currently the most
375 frequent storm types at this location. Further north at Sawtell and at Cape Byron, a typical
376 ETL drives a net southward potential sand transport rate of -1,200 and -3,200 m^3/hr,
377 respectively, which is in a reverse direction to the net northward regional longshore transport.
378 ETLs often form in an AI circulation (Browning and Goodwin, 2013) and the latter can also
379 produce an equivalent net southward potential sand transport if the nearshore *MWD* is east-
380 north-easterly to east-south-easterly, similar to that calculated for ETL events (ie <110°). In
381 comparison, typical SSLs at Terrigal-Wamberal, Sawtell and Cape Byron drive a northward
382 potential sand transport rate of 6,500, 5,000 and 3,000 m^3/hr, respectively.

383 Overall, along the entire NSW coast, SSLs, ITLs and STLs enhance the headland 'sand
384 valve', promote connectivity in the regional longshore sediment transport, and maintain a
385 shoreline planform in dynamic equilibrium, whereas in northern NSW, ETLs (the most
386 frequent and longest duration extreme storms (with peak storm H_s > 5 m)) reduce
387 connectivity, potentially turn off the 'sand valve', and episodically reverse the net northward
388 sand transport.

389 5.2 Storm Type Control on the Headland Bypassing Mechanisms

390 Immediately downdrift of headlands, the dynamic stability and planform geometry of the
391 bay-beach ('southern hook of planform') shoreline and upper shoreface bathymetry are
392 dependent upon mean and storm wave obliquity, headland bypassing frequency, longshore
393 sand supply, and the bypassing pathway or mechanism. The observed headland-bypassing
394 mechanisms are discussed in Goodwin *et al.* (2013) and include: (i) headland-attached, rip-
395 head leakage bypassing on the upper shoreface between swash-aligned embayments (Short,

1999); (ii) headland-attached bar bypassing along obliquely aligned coasts (Zenkovich, 1964; Short, 1999; Silviera *et al.* 2011; Acworth and Lawson, 2012); (iii) downdrift, shoreface strand-bypassing along obliquely aligned coasts (Smith, 2001), also known as cross-embayment bypassing at an angle of ~60° from the diffraction point to the embayed, downdrift shoreline (Goodwin *et al.,* 2013); and (iv) offshore rip leakage to headland-attached sand bodies on the lower shoreface and inner shelf (Ferland, 1990).

To investigate the relationship between different storm types, headland bypassing and the stability of bay-beach shorelines, we modeled the spatial wave power gradient for the Terrigal-Wamberal (closed-leaky), and Byron Bay (open) embayments (Figure 11). The 5 kW/m contour (determined from wave modelling) was used to illustrate sand bypassing pathways under different storm types. The 5 kW/m contour was chosen as it best matched bypassing pathways and isobaths produced under different directional wave regimes observed at Byron Bay (Goodwin *et al*., 2013).

SSL storm waves produce a wave power gradient in the lee of the headland, where the 5 kW/m contour describes the approximate location of the oblique, strand-bypassing pathway across the upper shoreface, and landwards of this contour the upper shoreface and shoreline is protected from high storm wave power. In contrast, the ETL storm waves: (i) produce a quasi, shoreline parallel 5 kW/m contour within the surf zone, exposing the embayed coast to high storm wave power; (ii) eliminate the strand-bypassing pathway; (iii) reduce the efficiency of the headland-attached bar bypassing pathway; and, (iv) enhance the rip leakage of sediment from the littoral system to headland-attached offshore sand bodies on the lower shoreface. The processes associated with ETL storm events are an important factor in forcing shoreline recession trends on drift-aligned compartments that are manifest in increasing planform curvature, towards a static equilibrium planform when sand supply into the compartment approaches zero (after Hsu and Evans, 1989).

421 5.3 Implications of a Poleward-Shift in Storm Type Distribution under Tropical Expansion on
422 Future Regional Longshore Sand Transport

423 Both surface and upper atmospheric measurements of the extent of the tropics has identified
424 robust poleward trends in the widening of the Hadley Cell and expansion of the Tropics.
425 These indicators include the poleward shift of the STR or intensification of the Subtropical
426 Anticyclone in the East Australian region (Timbal and Drosdowsky, 2013), an intensification
427 of the tradewinds (Seidel *et al*., 2008, England *et al*., 2014) and a poleward contraction of the
428 mid-latitude westerlies (Marshall *et al*, 2003; Arblaster *et al*., 2011). In the past decade, the
429 shift towards the La Niña-like state of the Pacific Decadal Oscillation and Interdecadal
430 Pacific Oscillation (Allen *et al*., 2014) has enhanced the tradewind intensification, and may
431 be contributing to the recent Tropical Expansion trend (during La Niña the tropics widen by
432 ~1 to 2° compared to El Niño years, Lucas *et al.,* 2014). The Tropical Expansion trend is
433 most apparent during the equinoxes, which is of significance because of the warm season
434 (late summer to autumn) occurrence of high magnitude ETLs along the north coast NSW. A
435 signature of recent and near-future climate change is an increased frequency of easterly and
436 north-easterly trade-wind generated waves replacing the regular propagation of Southern
437 Tasman and Southern Ocean swell waves (Hemer *et al*., 2013, Mortlock and Goodwin,
438 2015).

439 In the 21st century, mean wave climate along the SEAS is predicted to rotate anticlockwise
440 with tropical expansion and a poleward intensification of the westerlies with no significant
441 change in annual net wave power (Mortlock and Goodwin, 2015). The poleward expansion of
442 the tropics, measured by either the mean Southern Hemisphere-STR latitude or the surface
443 precipitation minimum, indicate a rate of 0.2 to 0.5° latitude per decade since 1979 (~0.6 to
444 1.5° total, Lucas *et al.,* 2014). A further poleward expansion of the tropics by ~1 to 2° is
445 projected during the 21st century (Lucas *et al.,* 2014). There is considerable regional

446 variability in the estimates of tropical expansion across the Southern Hemisphere.
447 Accordingly, we investigated the impact of a generalised, 2 to 2.5° poleward expansion of the
448 Tropics (since ~1979) on storm type distribution and impacts for headland bypassing and
449 regional longshore sand transport.

450 A 2 to 2.5° poleward shift in the STR would result in a comparable latitudinal shift in the
451 location of storm generation and wave propagation patterns, shown in Figures 5 and 6 for the
452 present. Under this scenario, there could be an increase in ETL/AI-generated storm waves in
453 the Central to Northern Tasman Sea. Whilst previous studies using GCM projections such as
454 Dowdy *et al* (2014) and Abbs and McInnes (2004) indicate a decline in East Coast Low
455 storm events later this century, there remains the risk of an increase in infrequent but high
456 magnitude storm wave events such as ex-TC, autumn to early winter ETLs forming at more
457 southerly latitudes, and an increase in AI.

458 To simulate a 2 to 2.5° poleward shift in the subtropics, we used a similar logic to that
459 described in Mortlock and Goodwin (2015) for the poleward migration of modal wave
460 climate, by suggesting that modern storm wave parameters from more northerly buoys can be
461 used as surrogate data to project future storm wave impacts at higher latitudes. For example,
462 modern storm wave parameters recorded at Coffs Harbour (Mid North coast) may be a
463 suitable surrogate for future storm waves parameters in the Sydney region (Central coast),
464 ~2.5° latitude to the south. Accordingly, we refracted the present-day offshore storm wave
465 parameters for the ETL and SSL types as measured at the Byron Bay buoy (North coast) for
466 the Sawtell location (Mid-North coast) using MIKE21 SW, and similarly, the present-day
467 offshore storm wave parameters as measured at the Coffs Harbour buoy were refracted for
468 the Terrigal-Wamberal location.

469 On the Central Coast at Terrigal-Wamberal, we simulate future longshore sand transport rates
470 for an ETL event to drive a net southward transport of 4,600 m^3/hr at the storm-peak, rather
471 than the present northward transport rate of 8,400 m^3/hr. To compound the transport reversal
472 for ETL events, there is a 30% reduction in the net northward transport rates for SSL events.
473 There is no change in the longshore sand transport rate for STLs (4,500 m^3/hr) compared to
474 present. At Sawtell, there is no change in future longshore sand transport rates for an ETL.
475 The rate for a typical SSL at Sawtell will increase by 16% to 5,800 m^3/hr but will be
476 associated with a 40% decrease in northward transport from STLs. Hence, we simulate a
477 reduction in the magnitude of episodic headland sand bypassing during ETL and SSL storm
478 events along the Central Coast of NSW, and slightly increased for SSL/ITL storm events and
479 reduced for STL events along the Mid North Coasts, for a ~2.5° poleward shift of the STR.
480 However, in both cases, an increase in the frequency of ETL events with a 2 to 2.5° poleward
481 shift in the subtropics would lead to a significant net southward sand transport component.

482 Since the strike of the shelf along the south-east Queensland coast (Brisbane Buoy) receives
483 significantly less storm wave energy from SSLs, the application of the Brisbane Buoy data as
484 surrogate data for future Byron Bay storm wave climate is not straight-forward. However, in
485 accordance with the seasonal difference in summer and winter STR (~4° latitude) and wave
486 climate at Brisbane and Byron Bay, we infer from the relative frequency of each storm type
487 between buoy locations that a 60% reduction in SSL driven longshore transport, together with
488 and at least ~5% increase in ETL driven net southward longshore transport events, is most
489 plausible. The combined impact of these changes to the storm wave climate in northern NSW
490 is a significant projected reduction in northward longshore sand transport and in the
491 efficiency of headland bypassing events.

492

6. CONCLUSIONS

The decomposition of Tropical Cyclone and East Coast Low storms into synoptic types is a necessary first step to determine the impact of a changing climate on storm-driven longshore sand transport along the Southeast Australian Shelf.. The results show that tropical origin storms (ETL, AI, TC and TL) produce a shore-normal propagation pattern along the SEAS, whilst the extratropical origin storms (STL/SSL/CL) and the hybrid storms (ITL) produce a shore-oblique propagation pattern from the Southern Tasman to the Coral Sea. The directional obliquity (clockwise of shore-normal orientation) of the extratropical origin waves (STL/SSL/CL) is an important control on the connectivity of regional longshore sand transport through episodic major headland bypassing events between compartments, and the maintenance of down-coast coastlines in dynamic equilibrium. In contrast, the direction of tropical origin waves (ETL/AI/TC/TL) is shore-normal or anticlockwise of shore-normal, and reduces the connectivity through minor headland bypassing events or episodically reversing the net northward transport.

Future climate change projections indicate that the recent trend in the expansion of the latitudinal extent of the tropics (defined at the surface by the latitude of the STR) in the south-west Pacific region will continue throughout this century. This will lead to a latitudinal shift in the synoptic type of storm wave generation and propagation. We find that a 2.5° poleward migration of the STR (as projected in some GCMs) may result in the SEAS experiencing a significant change in both the magnitude and alongshore direction of the potential longshore sand transport rate for each major storm type along the NSW coast. On the Central Coast, we project a reversal in the direction of ETL driven longshore sand transport rates of ~150%, with a further ~30% reduction in the potential net northward longshore sand transport associated with changes to SSL storms. North of Coffs Harbour to southeast Queensland, we project a 40% reduction in northward longshore sand transport

518 rates for SSL/STL events, together with at least a ~5% increase in reversed (net southward)
519 longshore sand transport for ETL events, north of Coffs Harbour to southeast Queensland.
520 There is the potential for northward sand transport rates along the central to mid-north coast
521 from SSL/ITL events to be un-changed. Overall, a projected latitudinal shift in synoptic
522 storm events could lead to a significant reduction in net northward longshore sand transport
523 and the efficiency of headland bypassing events. The potential byproduct of these impacts
524 will be planform recession and increased curvature towards the limiting static equilibrium
525 planform (after Hsu and Evans, 1989).

526 There remains the possibility for a net reversal (reduction) of the East Australian Longshore
527 sand transport system north (south) of ~29°S as a combined result of the anticlockwise
528 rotation in the mean wave field, together with the projected increase in ETLs and decrease in
529 SSLs. There is prior evidence for such a decline or 'turning-off the sand valve' and the
530 connected Australian longshore sediment transport system during the previous Quaternary
531 Interglacials with shifts to a dominant tradewind generated wave climate during the Last
532 Interglacial. Our results are also directly applicable to investigating the potential changes
533 along the other Southern Hemisphere east coasts, particularly along the Southern Brazil and
534 Natal to Mozambique regions.

535

536 ACKNOWLEDGEMENTS

537 Wave data from all NSW buoys is funded by NSW Office of Environment and Heritage
538 (OEH) and is operated by Manly Hydraulics Laboratory (MHL). Wave data from the
539 Brisbane buoy is funded by State of Queensland, Department of Science, Information
540 Technology, Innovation and the Arts (DSITIA) and distributed by Coastal Impacts Unit -
541 Science Delivery Division, DSITIA. Nearshore buoy deployments in the Sydney region and

542 at Sawtell Beach were funded by Australian Research Council (ARC) Linkage Project
543 (LP100200348) and data is available from the authors on request. Thanks to Sonny Tisdell
544 and Sawtell SLS Club for help with buoy deployments at Sawtell Beach. All bathymetry used
545 for refraction modelling was supplied by NSW OEH. A Macquarie University (MQU)
546 academic license for MIKE by DHI software was used. TRM was funded by a MQU
547 International Research Excellence Scholarship (MQiRES) in association with ARC
548 LP100200348. This paper is a contribution to the Eastern Seaboard Climate Change Initiative
549 – East Coast Lows (ESCCI-ECL) Project 4, and an NSW OEH and NSW Environmental
550 Trust Grant to IDG. We thank Tom Shand for his contribution to earlier drafts of this paper.
551 Deepwater (nearshore) spectral and parametric wave data used in this study can be obtained
552 from Mark.Kulmar@mhl,nsw.gov.au (ian.goodwin@mq.edu.au) respectively. All processed
553 wave data, the storm wave database, and wave refraction modeling data can be obtained from
554 ian.goodwin@mq.edu.au, or thomas.mortlock@mq.edu.au. The storm wave typology
555 database is available at http://mq.edu.au/mqmarine/data/SEAus_storm_wave .

556

557 REFERENCES

558 Abbs, D.J., and K.L. McInnes (2004), The impact of climate change on extreme rainfall and
559 coastal sea levels over south-east Queensland. Part 1, Analysis of extreme rainfall and wind
560 events in a GCM. A project undertaken for the Gold Coast City Council, CSIRO
561 Atmospheric Research. Aspendale, Victoria, 48 pp.

562 Acworth, C. and S. Lawson (2012), The Tweed River Entrance Sand Bypassing Project, ten
563 years of managing operations in a highly variable coastal system. Proceedings of the 20th
564 NSW Coastal Conference 2012 Tweed Heads, 1-23.

565 Allen, R. J., Norris, J. R., & Kovilakam, M. (2014), Influence of anthropogenic aerosols and

566 the Pacific Decadal Oscillation on tropical belt width. Nature Geoscience , 7(4), 270-274.

567 Arblaster, J. M., Meehl, G. A., & Karoly, D. J. (2011), Future climate change in the Southern
568 Hemisphere: Competing effects of ozone and greenhouse gases. Geophysical Research
569 Letters , 38(2), L02701.

570 Bertin, X., E. Prouteau and C. Letetrel (2013), A significant increase in wave height in the
571 North Atlantic Ocean over the 20th century. Global and Planetary Change 106: 77-83,
572 doi:10.1016/j.gloplacha.2013.03.009.

573 Bromirski, P. D., D. R. Cayan, J. Helly and P. Wittmann (2013), Wave power variability and
574 trends across the North Pacific. Journal of Geophysical Research: Oceans 118(12): 6329-
575 6348, doi:10.1002/2013JC009189.

576 Bromirski, P. D., and D. R. Cayan (2015), Wave power variability and trends across the
577 North Atlantic influenced by decadal climate patterns, Journal Geophysical Research:
578 Oceans, 120, doi:10.1002/2014JC010440.

579 Browning, S. A. and I. D. Goodwin (2013), Large-scale influences on the evolution of winter
580 Subtropical maritime cyclones affecting Australia's East Coast. Monthly Weather Review
581 141(7): 2416-2431, doi: 10.1175/MWR-D-12-00312.1.

582 Boyd, R., Ruming, K, Goodwin, I., Sandstrom, and M., Schroeder-Adams, C. (2008),
583 Highstand transport of coastal sand to the deep ocean: a case study from Fraser Island,
584 southeast Australia. Geology, 36 (1): 15-18, doi: 10.1130/G24211A.1.

585 Brocca, L., S. Hasenauer, T. Lacava, F. Melone, T. Moramarco, W. Wagner, W. Dorigo, P.
586 Matgen, J. Martínez-Fernández, P. Llorens, J. Latron, C. Martin and M. Bittelli (2011), Soil
587 moisture estimation through ASCAT and AMSR-E sensors: An intercomparison and

588 validation study across Europe. Remote Sensing of Environment, 115 (12): 3390-3408,
589 doi:10.1016/j.rse.2011.08.003.

590 Cai, W., G. Shi, T. Cowan, D. Bi and J. Ribbe (2005), The response of the Southern Annular
591 Mode, the East Australian Current, and the southern mid-latitude ocean circulation to global
592 warming. Geophysical Research Letters 32, L23706, doi:10.1029/2005GL024701.

593 Coghlan, I., M. A. Mole, T. D. Shand, J. T. Carley, W. L. Peirson, B. Miller, M. Kulmar, E.
594 Couriel, B. Modra and B. You (2011), High resolution wave modelling (HI-WAM) for
595 Batemans Bay detailed wave study. Proceedings of the 20th Australasian Coastal and Ocean
596 Engineering Conference, Institution of Engineers Australia, Perth, Australia, 215 – 221.

597 Dee, D. P., S. M. Uppala, A. J. Simmons, P. Berrisford, P. Poli, S. Kobayashi, U. Andrae, M.
598 A. Balmaseda, G. Balsamo, P. Bauer, P. Bechtold, A. C. M. Beljaars, L. van de Berg, J.
599 Bidlot, N. Bormann, C. Delsol, R. Dragani, M. Fuentes, A. J. Geer, L. Haimberger, S. B.
600 Healy, H. Hersbach, E. V. Hólm, L. Isaksen, P. Kållberg, M. Köhler, M. Matricardi, A. P.
601 McNally, B. M. Monge-Sanz, J. J. Morcrette, B. K. Park, C. Peubey, P. de Rosnay, C.
602 Tavolato, J. N. Thépaut and F. Vitart (2011), The ERA-Interim reanalysis: configuration and
603 performance of the data assimilation system. Quarterly Journal of the Royal Meteorological
604 Society 137(656): 553-597, doi: 10.1002/qj.828.

605 del Valle, R., R. Medina, and M.A. Losada (1993), Dependence of the Coefficient *K* on the
606 Grain Size. J. Waterway, Port, Coastal and Ocean Eng., ASCE, 118, 6, 568–574.

607 DHI (2014), MIKE21 SW Spectral Wave Model FM User Guide, MIKE by DHI, Danish
608 Hydraulics Institute, Denmark, 122 pp.

609 Dowdy, A. J., G. A. Mills, B. Timbal and Y. Wang (2014), Fewer large waves projected for
610 eastern Australia due to decreasing storminess. Nature Climate Change 4(4): 283-286, doi:
611 10.1038/nclimate2142.

612 Drosdowsky, W. (2005), The latitude of the subtropical ridge over Eastern Australia: The L
613 index revisited. International Journal of Climatology 25(10): 1291-1299, doi:
614 10.1002/joc.1196.

615 England, M. H., S. McGregor, P. Spence, G. A. Meehl, A. Timmermann, W. Cai, A. S.
616 Gupta, M. J. McPhaden, A. Purich, A. Santoso , (2014), Recent intensification of wind-
617 driven circulation in the Pacific and the ongoing warming hiatus. Nat Clim Chang 4(3):222–
618 227.

619 Ferland, M. A. (1990), Shelf sand bodies in southeastern Australia, unpublished PhD thesis,
620 Department of Geography, University of Sydney, NSW, Australia.

621 Goodwin, I. D. (2005), A mid-shelf, mean wave direction climatology for southeastern
622 Australia, and its relationship to the El Niño—Southern Oscillation since 1878A.D.
623 International Journal of Climatology 25(13): 1715-1729, doi: 10.1002/joc.1207.

624 Goodwin, I. D., R. Freeman and K. Blackmore (2013), An insight into headland sand
625 bypassing and wave climate variability from shoreface bathymetric change at Byron Bay,
626 New South Wales, Australia. Marine Geology 341: 29-45,
627 doi:10.1016/j.margeo.2013.05.005.

628 Harley, M. D., I. L. Turner, A. D. Short and R. Ranasinghe (2010), Interannual variability
629 and controls of the Sydney wave climate. International Journal of Climatology 30(9): 1322-
630 1335, doi: 10.1002/joc.1962.

631 Hemer, M. A. (2010), Historical trends in Southern Ocean storminess: Long-term variability
632 of extreme wave heights at Cape Sorell, Tasmania. Geophysical Research Letters 37(18):
633 l18601, doi:10.1029/2010gl044595.

634 Hemer, M. A., J. Katzfey and C. E. Trenham (2013), Global dynamical projections of surface
635 ocean wave climate for a future high greenhouse gas emission scenario. Ocean Modelling 70:
636 221-245, doi:10.1016/j.ocemod.2012.09.008.

637 Holthuijsen, L. H. (2007), Waves in oceanic and coastal waters. Cambridge University Press,
638 Cambridge, U.K. pp 387.

639 Hsu, J.R.C. and Evans, C. (1989), Parabolic bay shapes and applications. Proceedings,
640 Institution of Civil Engineers, 87(2), 557–570.

641
642 Kalnay, E., M. Kanamitsu, R. Kistler, W. Collins, D. Deaven, L. Gandin, M. Iredell, S. Saha,
643 G. White, J. Woollen, Y. Zhu, M. Chelliah, W. Ebisuzaki, W. Higgins, J. Janowiak, K. C.
644 Mo, C. Ropelewski, J. Wang, A. Leetmaa, R. Reynolds, R. Jenne and D. Joseph (1996), The
645 NCEP/NCAR 40-year reanalysis project. Bulletin of the American Meteorological Society
646 77(3): 437-471, doi: 10.1175/1520-0477(1996)077<0437:TNYRP>2.0.CO;2.

647 Komar, P. D. and J. C. Allan (2008), Increasing hurricane-generated wave heights along the
648 US East Coast and their climate controls. Journal of Coastal Research 24(2): 479-488, doi:
649 10.2112/07-0894.1.

650 Kulmar, M., B. Modra and M. Fitzhenry (2013), The New South Wales wave climate
651 improved understanding through the introduction of directional wave monitoring buoys.
652 Proceedings of the Coasts and Ports Conference, 11-13 September, 2012.

653 Lucas, C. Timbal, B. and Nguyen, H. (2014), The expanding tropics: a critical assessment of
654 the observational and modeling studies. WIREs Clim Change 2014, 5:89–112. doi:
655 10.1002/wcc.251

656 Mortlock, T. R. and I. D. Goodwin (2015), Directional wave climate and power variability
657 along the Southeast Australian Shelf. Continental Shelf Research, 98: 36-53,

658 doi:10.1016/j.csr.2015.02.007.

659 Peixoto, J. and A. Oort (1992), Physics of Climate, American Institute of Physics, New York,
660 USA, pp 520.

661 Pittock A.B. (1973), Global meridional interactions in stratosphere and troposphere.
662 Quarterly Journal of the Royal Meteorological Society 99(421): 424–437.

663 PWD (1985), Elevated ocean levels – Storms affecting the NSW coast 1880-1980. Report
664 prepared by Blain, Bremner and Williams Pty. Ltd, for the NSW Public Works Department
665 Coastal Branch in conjunction with Weatherex Meteorological Services, PWD Report No.
666 85041

667 PWD (1986), Elevated ocean levels – Storms affecting the NSW coast 1980-1985. . Report
668 prepared by Lawson and Treloar Pty. Ltd. for the NSW Public Works Department Coastal
669 Branch, in conjunction with Weatherex Meteorological Services, PWD Report No. 86026

670 Rosati, J.D., T.L. Walton, K. Bodge (2002), Longshore sediment transport. In: Vincent, L.,
671 and Demirbilek, Z. (editors), Coastal Engineering Manual, Part III, Chapter III-2, Engineer
672 Manual 1110-2-1100, U.S. Army Corps of Engineers, Washington, DC.

673 Roy, P.S. and Stephens, A.W. (1980), Regional geological studies of the N.S.W. inner
674 continental shelf summary results. Geological Survey Report No GS 1980/028. Geological
675 Survey of New South Wales, Department of Mines, Sydney Australia.

676 Ruggiero, P., P. D. Komar and J. C. Allan (2010), Increasing wave heights and extreme value
677 projections: The wave climate of the U.S. Pacific Northwest. Coastal Engineering 57(5): 539-
678 552, doi:10.1016/j.coastaleng.2009.12.005.

679 Seidel, D. J., Q. Fu, W. J. Randel and T. J. Reichler (2008), Widening of the tropical belt in a

680 changing climate. Nature Geoscience 1(1): 21-24, doi:10.1038/ngeo.2007.38.

681 Shand, T. D., I. D. Goodwin, M. A. Mole, J. T. Carley, S. A. Browning, I. Coghlan, M. D.
682 Harley and W. J. Pierson (2011), NSW Coastal Inundation Hazards Study: Coastal Storms
683 and Extreme Waves, Water Research Laboratory & Climate Futures at Macquarie University,
684 WRL Technical Report 2010/16, University of New South Wales, pp 75.

685 Short, A D, (ed), (1999), Beach and Shoreface Morphodynamics. John Wiley and Sons,
686 Chichester, 379 pp.

687 Silveira, L.F., Klein, A.H.da F. and Tessler, M.G. (2010), Headland-bay beach planform
688 stability of Santa Catarina State and of the northern coast of Sao Paulo State. Brazilian
689 Journal of Oceanography, 58(2), 101-122.

690 Smith, AW (2001), Headland bypassing. In: Coasts & Ports 2001: Proceedings of the 15th
691 Australasian Coastal and Ocean Engineering Conference, the 8th Australasian Port and
692 Harbour Conference. Barton, A.C.T.: Institution of Engineers, Australia, 2001, 214-216.

693 Speer, M. S., P. Wiles and A. Pepler (2009), Low pressure systems off the New South Wales
694 coast and associated hazardous weather: establishment of a database. Australian
695 Meteorological and Oceanographic Journal 58, 29-39.

696 Timbal, B. and Drosdowski, W., (2012), The relationship between the decline of Southern
697 Australian rainfall and the strengthening of the subtropical ridge. Int J. Climatology,
698 DOI:10.1002/joc.3492.

699 Thompson, D.W.J., S. Solomon (2002), Interpretation of recent Southern Hemisphere climate
700 change. Science 296: 895–899, doi:10.1126/science.1069270.

701 Wang, X. L., Y. Feng and V. R. Swail (2012), North Atlantic wave height trends as

reconstructed from the 20th century reanalysis. Geophysical Research Letters 39(18): L18705, doi: 10.1029/2012GL053381.

Whiteway, T.G. (2009), Australian bathymetry and topography grid. Geoscience Australia Report 2009/21. Australian Government. June 2009.

Young, I. R. (1999), Seasonal variability of the global ocean wind and wave climate. International Journal of Climatology 19(9): 931-950, doi: 10.1002/(SICI)1097-0088(199907)19:9<931::AID-JOC412>3.0.CO;2-O.

Zenkovich, V.P. (Ed. Steers, J.A.) (1967), Processes of coastal development. Oliver and Boyd, London, pp738.

713 TABLES

714 Table 1. Directional and non-directional buoy record used in this study. Water depths reflect
715 current moored position.

Wave Station (N to S)	**Latitude (decimal degrees)**	**Water Depth (m)**	**Date Site Commissioned**	**Directional Buoy Deployed**
Brisbane	- 27.48	70	31-Oct-1976	20-Jan-1997
Byron Bay	- 28.85	62	14-Oct-1976	26-Oct-1999
Coffs Harbour	- 30.35	72	26-May-1976	14-Feb-2012
Crowdy Head	- 31.81	79	10-Oct-1985	19-Aug-2011
Sydney	- 33.77	92	17-Jul-1987	03-Mar-1992
Botany Bay	- 34.04	75	08-Apr-1971	14-Jan-2015
Port Kembla	- 34.47	80	07-Feb-1974	20-Jun-2012
Batemans Bay	- 35.70	73	27-May-1986	23-Feb-2001
Eden	- 37.30	100	08-Feb-1978	16-Dec-2011

716

717

718 Table 2. Mid-shelf storm-peak parameters, mean frequency of occurrence and wave base for

719 the four most frequent storm types on the central, mid-north and north coast NSW.

Storm Type	**Frequency of occurrence (%)**	**Average Storm Peak H_s (m)**	**Average Storm Peak T_p (s)**	**Average Storm Peak *Dir* (°)**	**Wave Base for Storm Peak H_s (m)**
Sydney / Port Kembla					
STL	36	3.8	11.1	172	96
SSL	28	4.3	11.0	170	95
ITL	18	4.2	10.4	157	85
ETL	7	5.3	11.8	153	109
Coffs Harbour					
ITL	25	4.1	10.5	142	86
ETL	23	4.6	11.5	116	103
SSL	21	3.9	11.1	149	96
STL	14	3.6	11.3	161	100
Byron Bay					
SSL	26	3.8	11.1	167	96
AI	23	3.4	9.5	139	71
ITL	15	3.9	10.4	156	85
ETL	12	4.3	10.6	115	88

720

721

722 Table 3. Storm type definitions. Abbreviations of storm types are used throughout this paper.

Abbreviation	Full Name	Storm Description
TC	Tropical Cyclone	Swell related to named Tropical Cyclones forming in the Coral Sea between 5-10° latitude.
TL	Tropical Low	Low pressure systems forming in the Coral Sea but not reaching the low pressure intensity of a named tropical cyclone
AI	Anticyclone Intensification	Form when a high across the Tasman Sea directs onshore NE to SE winds to the coast
ETL	Easterly Trough Low	Cyclonic depressions generated primarily along the central NSW coast between 25° and 40° latitude
ITL	Inland Trough Low	Originate in the quasi-permanent low pressure trough over inland Qld, their movement to the east coast is often associated with STL
CL	Continental Low	Storms originating in Western Australia of the Great Australian Bight and moving overland, often re-intensify upon crossing the east coast
SSL	Southern Secondary Low	Form as a secondary cut off extratropical low in the Southern Tasman sea
STL	Southern Tasman Low	Major lows in the Southern Ocean south of 38°S

723

724

Table 4. Nearshore storm-peak wave parameters, wave obliquity and longshore transport rates (at ~ 5 m depth) for the present-day most frequent storm types at the three study sites. Present-day storm conditions at Byron Bay (Sawtell) were used as a surrogate for the Sawtell (Terrigal-Wamberal) compartment to represent a future southerly shift in storm wave climate with a 2 to 2.5 ° expansion of the tropics.

	Nearshore H_s (m)	**Nearshore *MWD* (°)**	**α (°)** *	***Q*** **(m^3/hr)** *
Terrigal-Wamberal (present-day)				
ETL	4.7	117	7	+ 8,400
ITL	3.8	119	9	+ 6,300
SSL	3.7	120	10	+ 6,500
STL	3.3	119	9	+ 4,400
Terrigal-Wamberal (future scenario)				
ETL	4.6	106	-4	- 4,600
ITL	4.0	115	5	+ 4,000
SSL	3.9	116	6	+ 4,500
STL	3.5	118	8	+ 4,500
Sawtell (present-day)				
ETL	3.5	122	-2	- 1, 200
ITL	3.2	134	10	+ 4,600
SSL	3.1	136	12	+ 5,000
STL	2.9	139	15	+ 5,200
Sawtell (future scenario)				
ETL	3.3	122	-2	- 1,000
ITL	3.0	139	15	+ 5,600
SSL	2.9	141	17	+ 5,800
AI	2.9	133	9	+ 3,200
Byron Bay (present-day)				
ETL	3.2	105	- 7	- 3,200
ITL	2.8	121	9	+ 2,900
SSL	2.7	122	10	+ 3,000
AI	2.7	117	5	+ 1,500

* The nearshore wave obliquity, α, is positive (negative) if clockwise (anti-clockwise) of shore-normal, so that *Q* is positive (negative) for northward (southward) longshore transport. Given the sensitivity of *Q* to small errors in H_s and α, values are indicative only and rounded to the nearest 100 m^3.

743

744 FIGURE CAPTIONS

745 Figure 1. Location of mid-shelf wave buoys (red or black flags), study sites (green circles)
746 and prominent headlands (yellow arrows) on the south east coast of Australia. Red flags
747 indicate a part-directional wave buoy record that was used in this study, black symbols
748 indicate a non-directional record. Also shown is the direction of regional longshore sand
749 transport (south to north), driven by headland-rip leakage (dotted yellow line) and headland
750 sand bypassing.

751 Figure 2. *MWD* hindcast at Coffs Harbour by CDF matching using *MWD* at Byron Bay; a)
752 hourly observations of *MWD* (green) and quantiles (blue) at Coffs Harbour and Byron Bay
753 (Feb 2012 – Dec 2013), b) cumulative distribution and c) probability density of *MWD*
754 observed at Coffs Harbour and Byron Bay, and resultant hindcast at Coffs Harbour for 2000 –
755 2012.

756 Figure 3. Sites for refraction modelling of storm types and regional map. 2m spaced
757 bathymetry from 0m contour shown. Yellow circles (red flags) indicate nearshore (offshore)
758 buoy locations. A variable scale is used between sites due to differences in alongshore
759 compartment length. The 6, 12 and 30 m contours are highlighted at each site to denote the
760 approximate seaward extent of the surf zone, upper/lower shoreface and lower
761 shoreface/inner shelf boundary. Study sites are denoted as green circles in regional map.

762 Figure 4. MIKE21 SW model validation against Wamberal and Sawtell nearshore Directional
763 WaveRider buoy observations for a) wave height, b) wave period, c) wave direction and d)
764 wave power. Quantiles (blue crosses) and linear regression (red line) are shown with scatter
765 data. All verification metrics are given to $p < 0.05$.

766 Figure 5. MSLP anomaly (hPa) composites (using ERA-Interim daily data) for each synoptic
767 storm type. Black dots show the location of the maximum MSLP within the study area (box

768 shown 10° - 44° S and 145° - 150° E) during each individual event (day) within the storm
769 type cluster and are indicative of the location of the Subtropical Ridge (note that due to grid
770 resolution multiple events may be plotted over the same location). Grey cross indicates the
771 mean location for all events with 1σ error bars.
772 Figure 6. Composite storm wave propagation patterns in the Tasman and Coral Seas using
773 ERA-Interim hindcast wave data (1980 – 2011) for each of the eight synoptic storm types
774 defined in Figure 5.
775 Figure 7. Latitudinal (A) distribution of storm types and (B) gradient in storm wave direction
776 (for (A), Sydney includes Botany Bay buoy record).
777 Figure 8. Refraction patterns for the four most commonly-occurring storm types at Terrigal-
778 Wamberal, showing gradients in P_0 and vectors of *MWD*. The peak-storm *MWD* (offshore)
779 and mean percentage occurrence of each storm type are shown. The approximate nearshore
780 headland location for calculation of updrift longshore sand transport, Q, is also shown (black
781 circle). The strike of the coast (black arrow) and shore-normal wave direction (dotted line)
782 that were used to estimate nearshore wave obliquity, α, are also shown. Storm types are
783 ordered following a clockwise rotation of *MWD* (top left to bottom right).
784 Figure 9. Refraction patterns for the four most commonly-occurring storm types at Sawtell
785 (as Figure 8).
786 Figure 10. Refraction patterns for the four most commonly-occurring storm types at Byron
787 Bay (as Figures 8 and 9).
788 Figure 11. Difference between Southern Secondary Low (SSL) and Easterly Trough Low
789 (ETL) storm wave propagation patterns on the SEAS (A), and 5 kW/m nearshore wave power
790 gradients (B) in headland shadow zones at Terrigal-Wamberal and Byron Bay. Arrows in (B)
791 represent the centroid peak storm mid-shelf wave direction for SSL (white) and ETL (red) at

Sydney (for Terrigal-Wamberal) and Byron Bay buoys. The dotted white line at Byron Bay illustrates the 5 kW/m power gradient for SSL without the shadowing effect of Julian Rocks.

Figure 12. Conceptual representation of present-day and future storm-driven longshore sand transport along the SEAS for ETL and SSL/STL storm events in response to a 2 to 2.5° poleward tropical expansion scenario. Black (yellow) arrows represent the present-day (future) direction and magnitude of longshore sand transport for typical ETL and SSL storms.

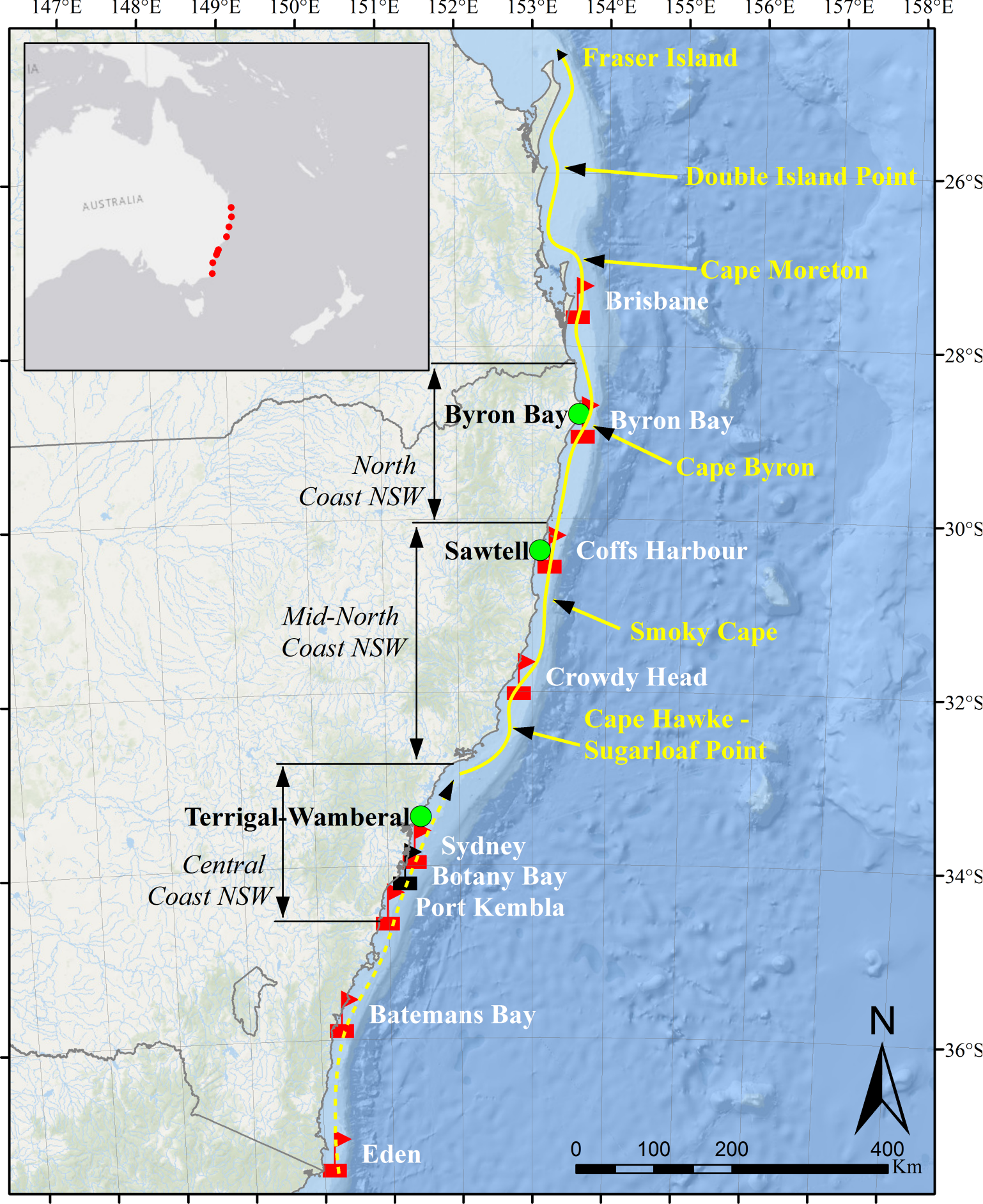
147°E
148°E
149°E
150°E
151°E
152°E
153°E
154°E
155°E
156°E
157°E
158°E
26°S
28°S
30°S
32°S
34°S
36°S
AUSTRALIA
Fraser Island
Double Island Point
Cape Moreton
Brisbane
Byron Bay
Byron Bay
Cape Byron
North
Coast NSW
Sawtell
Coffs Harbour
Mid-North
Coast NSW
Smoky Cape
Crowdy Head
Cape Hawke -
Sugarloaf Point
Terrigal-Wamberal
Sydney
Botany Bay
Port Kembla
Central
Coast NSW
Batemans Bay
Eden
N
0
100
200
400
Km

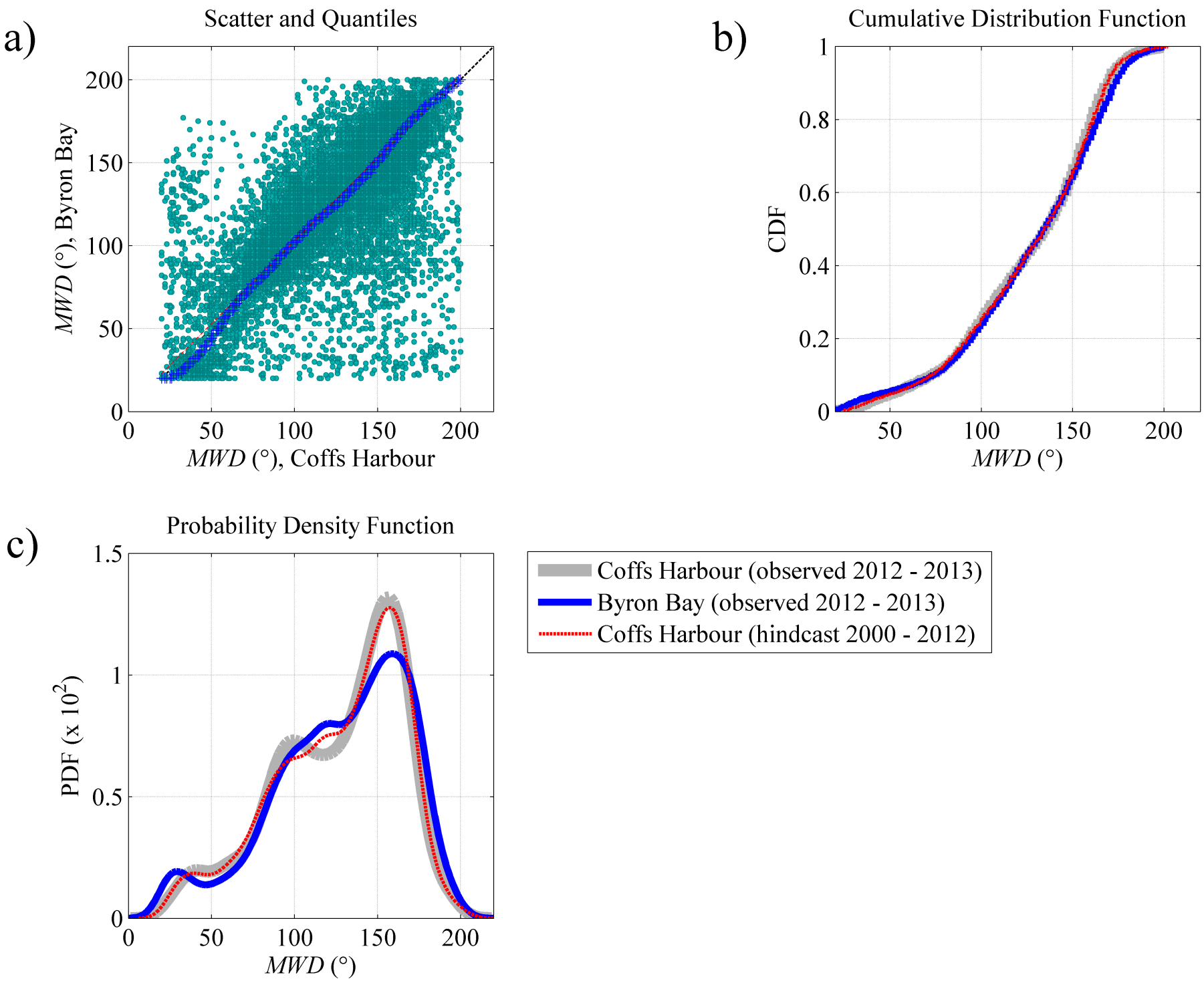
a)
Scatter and Quantiles
MWD (°), Byron Bay
MWD (°), Coffs Harbour
0
50
100
150
200
b)
Cumulative Distribution Function
CDF
MWD (°)
0
0.2
0.4
0.6
0.8
1
c)
Probability Density Function
PDF (x 10^2)
MWD (°)
0
0.5
1
1.5
Coffs Harbour (observed 2012 - 2013)
Byron Bay (observed 2012 - 2013)
Coffs Harbour (hindcast 2000 - 2012)

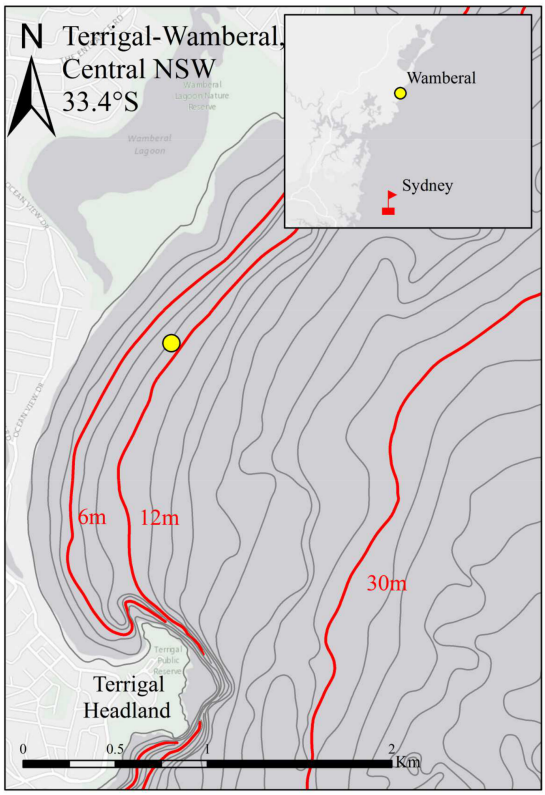
N
Terrigal-Wamberal,
Central NSW
33.4°S
Wamberal
Sydney
6m
12m
30m
Terrigal
Headland
0
0.5
1
2
Km

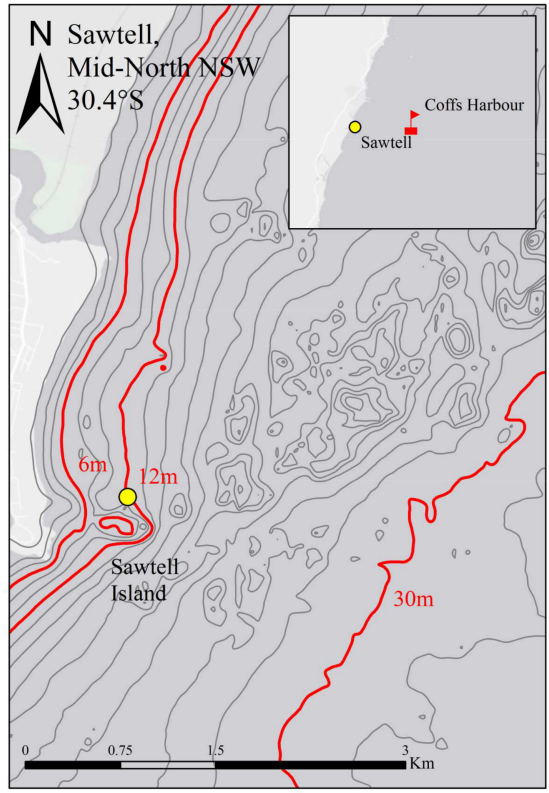
N
Sawtell,
Mid-North NSW
30.4°S
Coffs Harbour
Sawtell
6m
12m
Sawtell
Island
30m
0
0.75
1.5
3
Km

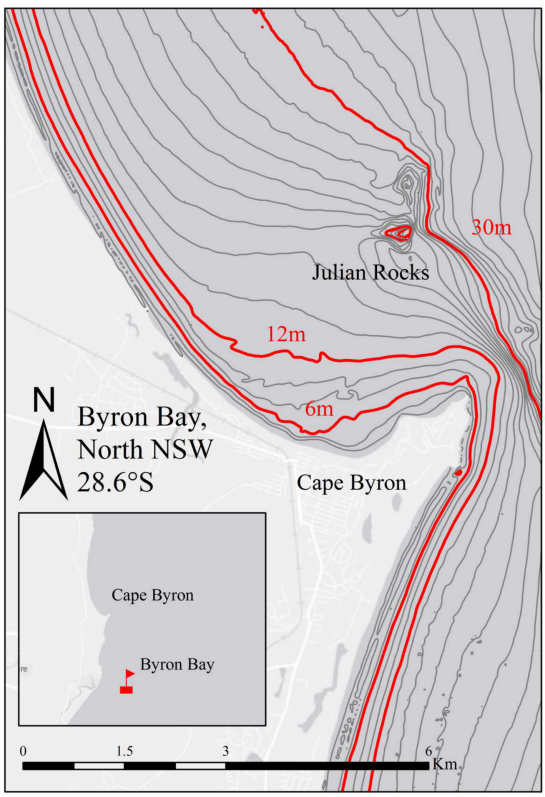
N
Byron Bay,
North NSW
28.6°S
30m
Julian Rocks
12m
6m
Cape Byron
Cape Byron
Byron Bay
0
1.5
3
6
Km

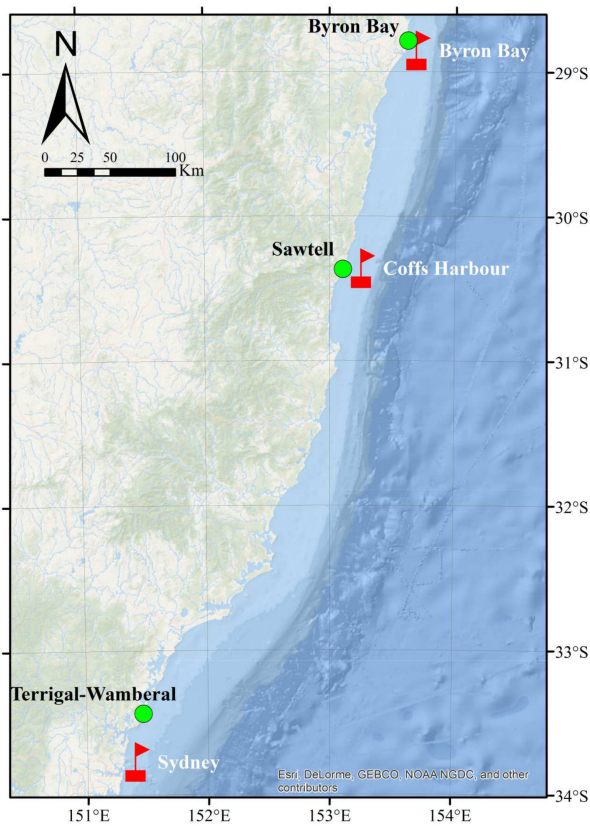
N
0
25
50
100
Km
Byron Bay
Byron Bay
Sawtell
Coffs Harbour
Terrigal-Wamberal
Sydney
Esri, DeLorme, GEBCO, NOAA NGDC, and other contributors
29°S
30°S
31°S
32°S
33°S
34°S
151°E
152°E
153°E
154°E

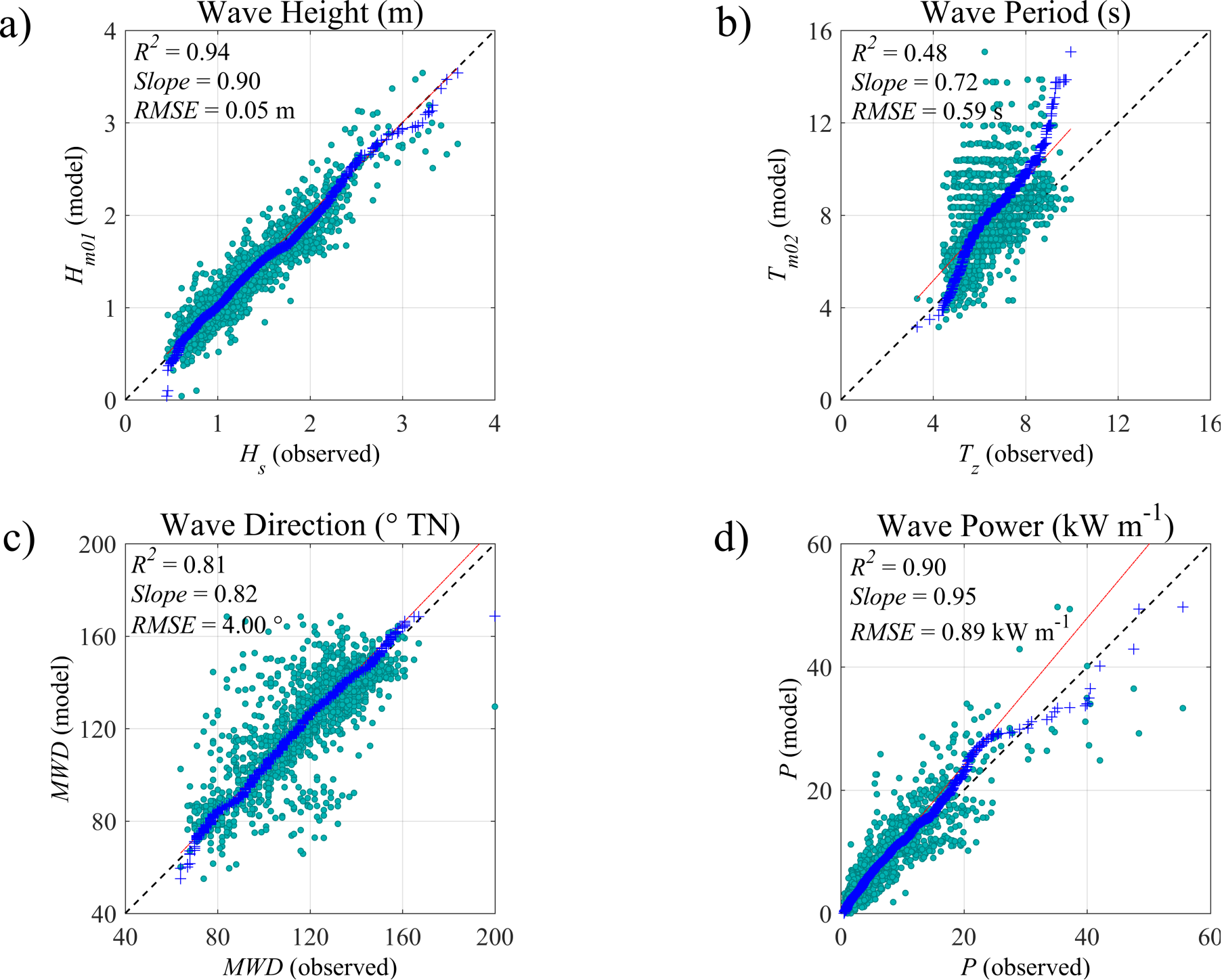
a)
Wave Height (m)
R^2 = 0.94
Slope = 0.90
RMSE = 0.05 m
H_{m01} (model)
H_s (observed)
b)
Wave Period (s)
R^2 = 0.48
Slope = 0.72
RMSE = 0.59 s
T_{m02} (model)
T_z (observed)
c)
Wave Direction (° TN)
R^2 = 0.81
Slope = 0.82
RMSE = 4.00 °
MWD (model)
MWD (observed)
d)
Wave Power (kW m^{-1})
R^2 = 0.90
Slope = 0.95
RMSE = 0.89 kW m^{-1}
P (model)
P (observed)

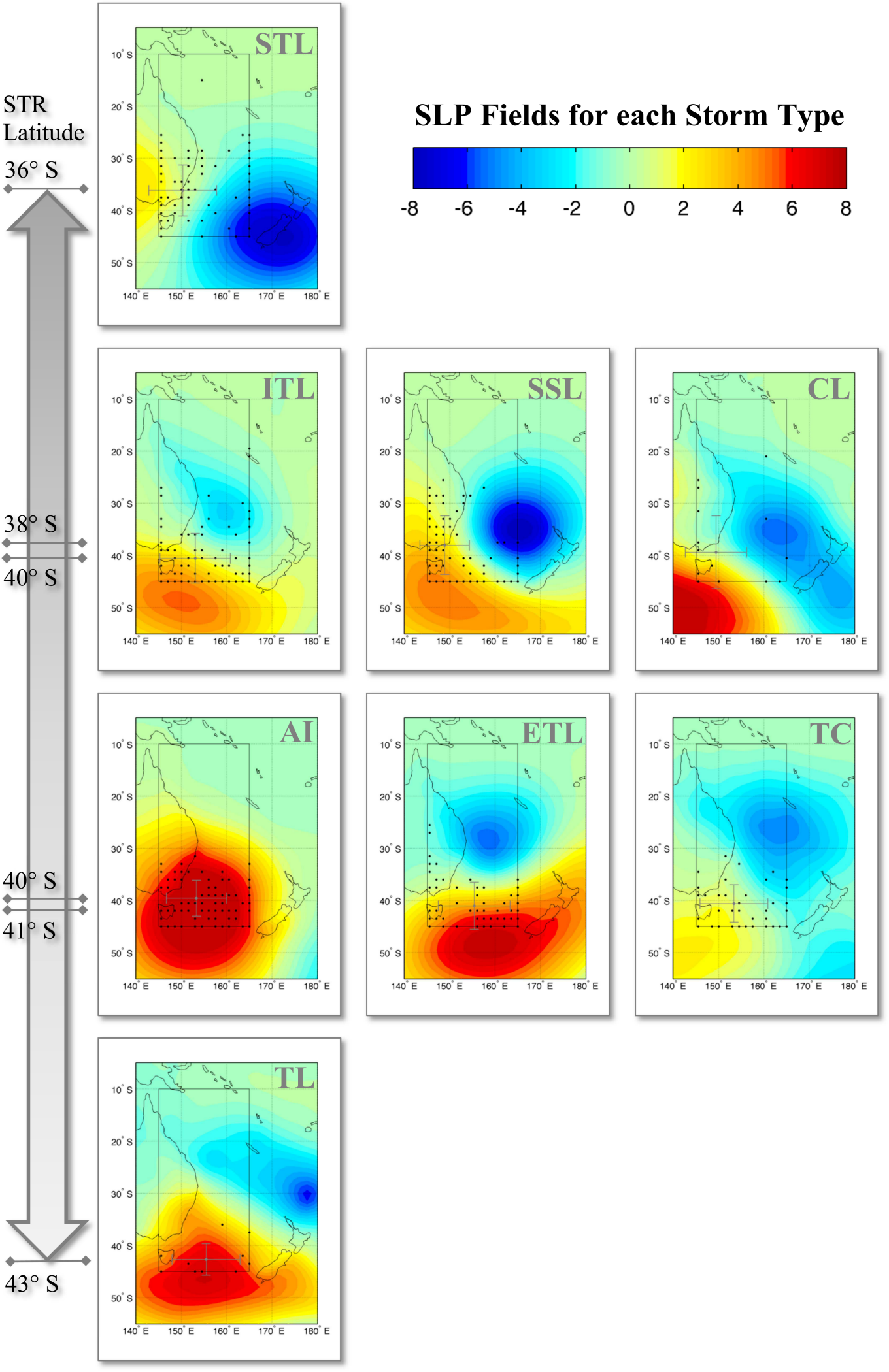
SLP Fields for each Storm Type
-8 -6 -4 -2 0 2 4 6 8
STR Latitude
36° S
38° S
40° S
40° S
41° S
43° S
STL
ITL
SSL
CL
AI
ETL
TC
TL
10° S
20° S
30° S
40° S
50° S
140° E
150° E
160° E
170° E
180° E

Storm wave propagation patterns

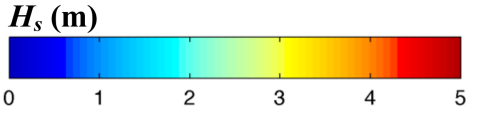

A. STL
(n = 224)

B. SSL
(n = 187)

C. CL
(n = 23)

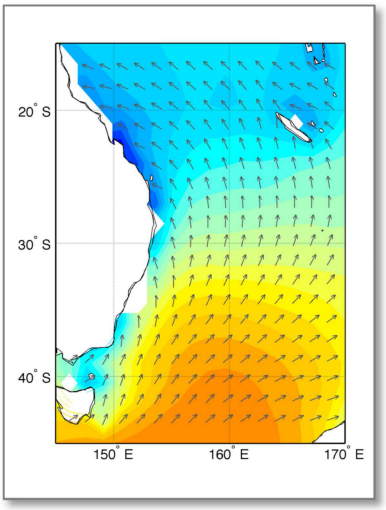

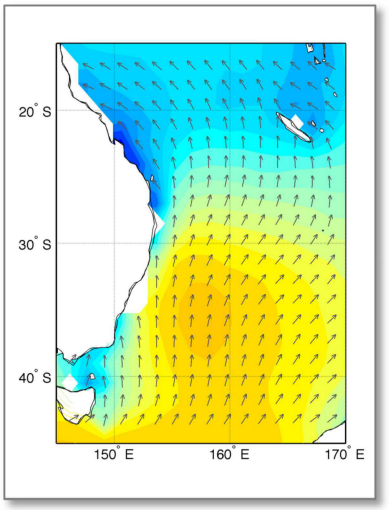

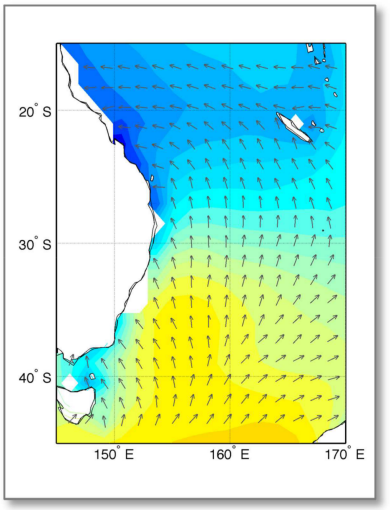

D. ETL
(n = 94)

E. ITL
(n = 180)

F. TC
(n = 63)

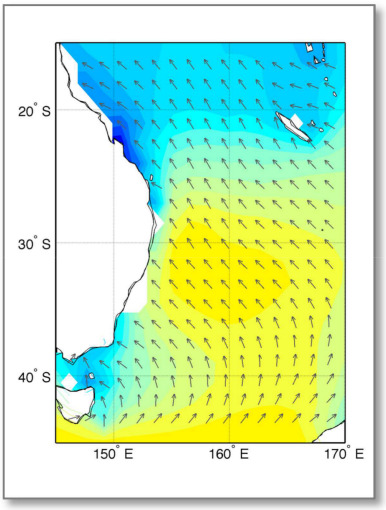

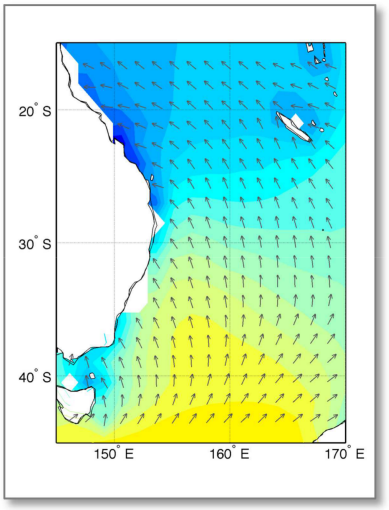

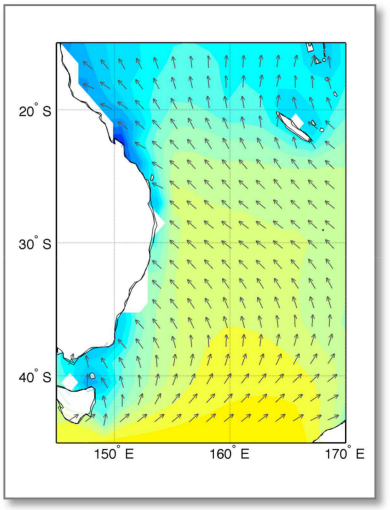

G. TL
(n = 11)

H. AI
(n = 116)

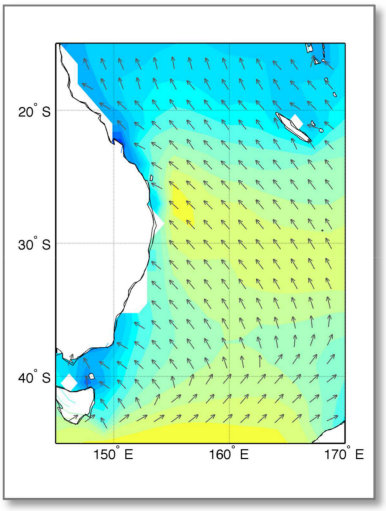

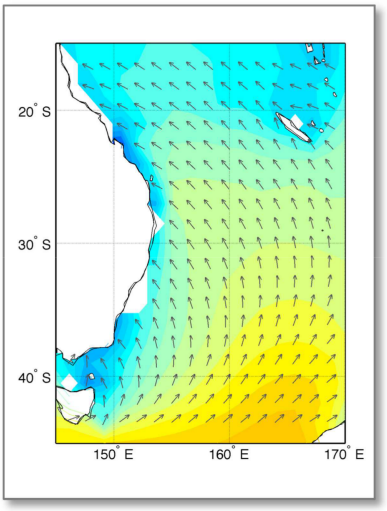

A. Latitudinal distribution of storm types

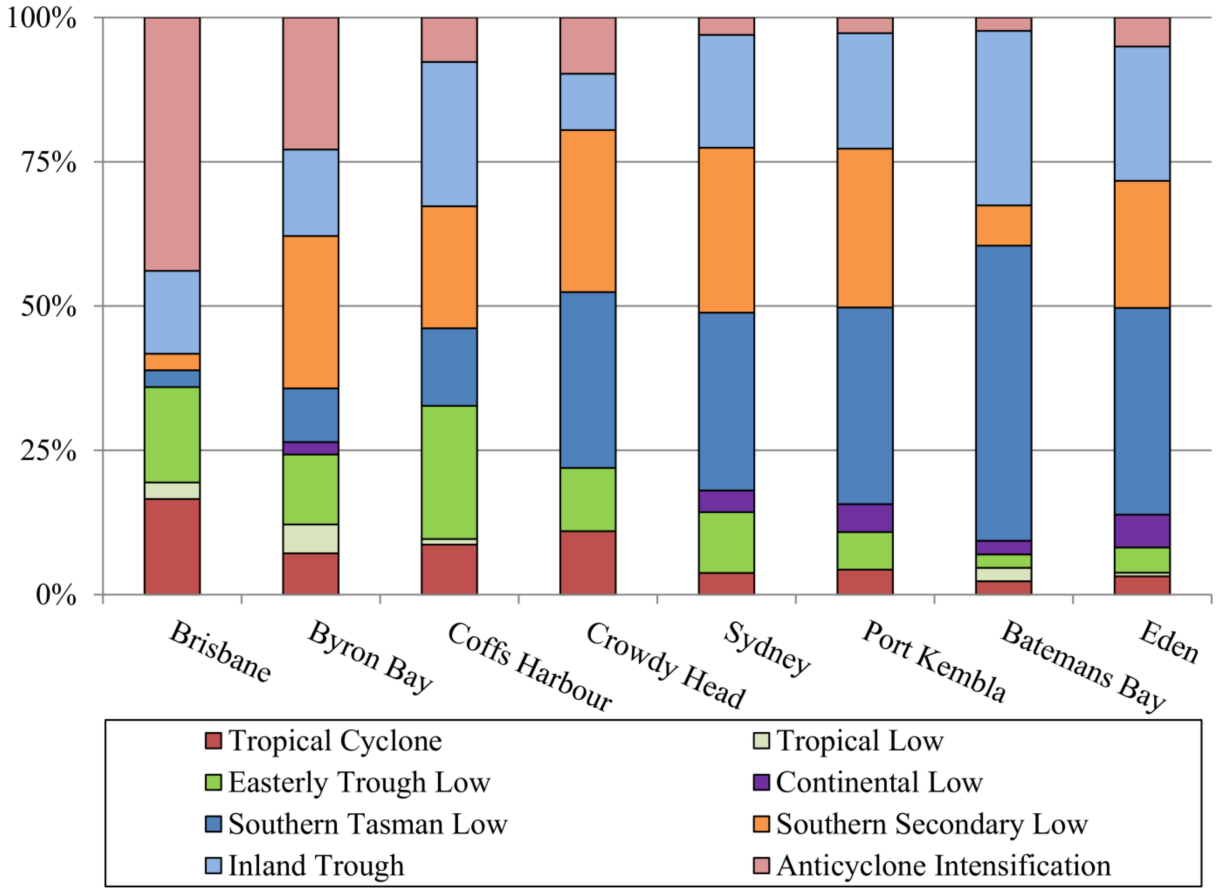

B. Latitudinal gradient in storm wave direction (1-hourly H_s > 3.0m)

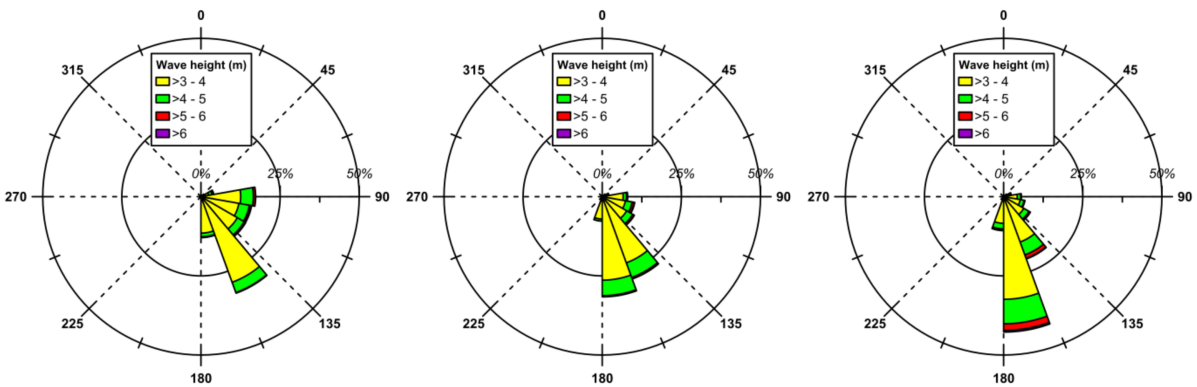

Brisbane (1997 – 2013)

Byron Bay (2000 – 2013)

Sydney (1992 – 2013)

Terrigal-Wamberal (Central Coast NSW)

ETL (153°, 7%)

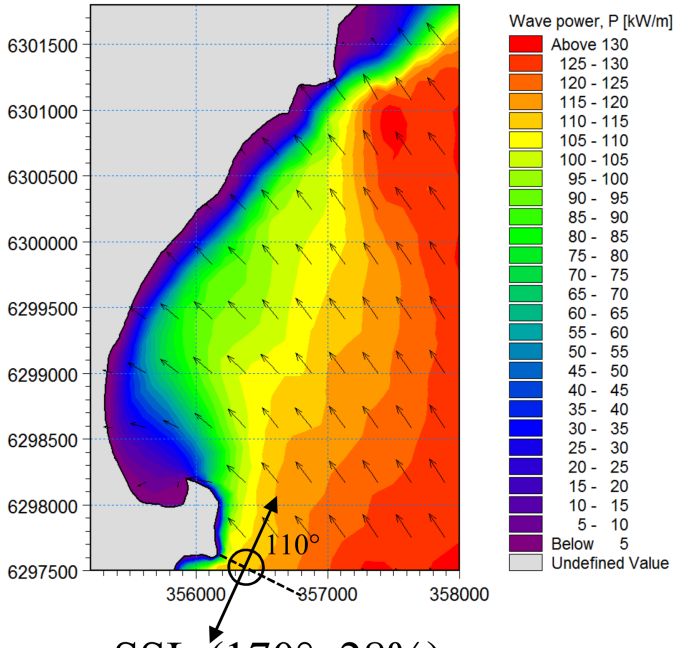

ITL (157°, 18%)

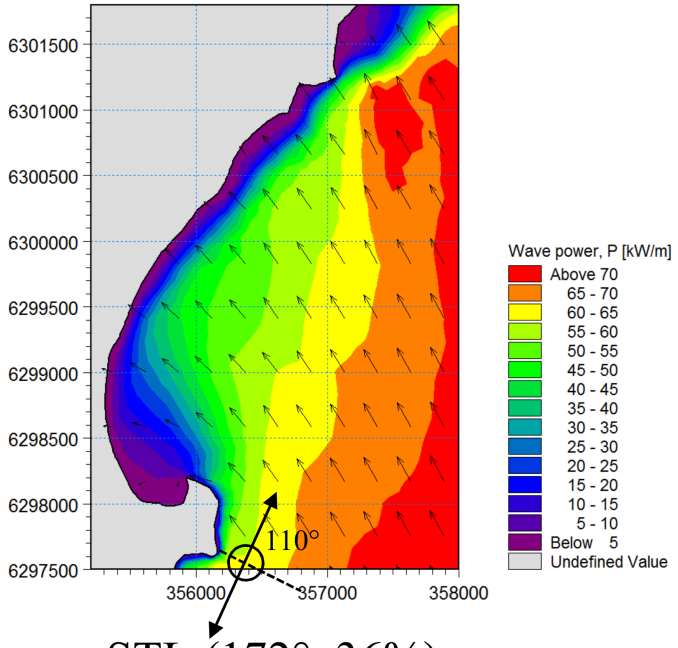

SSL (170°, 28%)

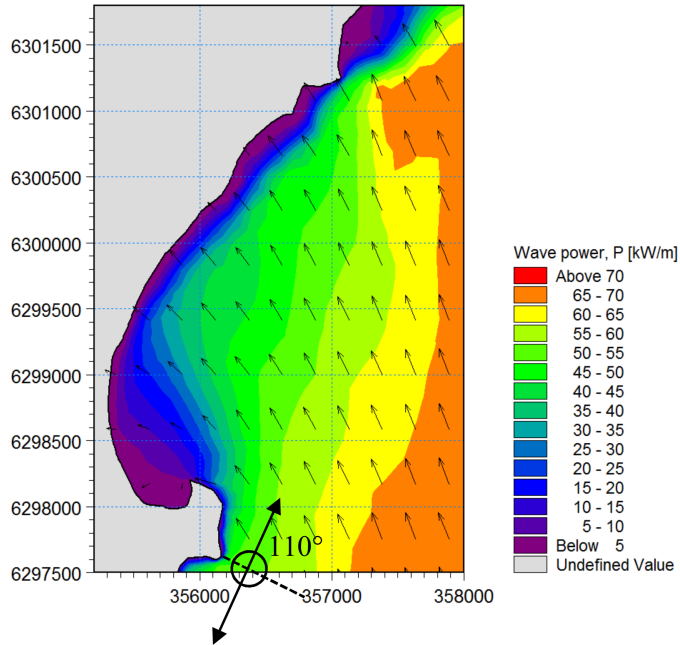

STL (172°, 36%)

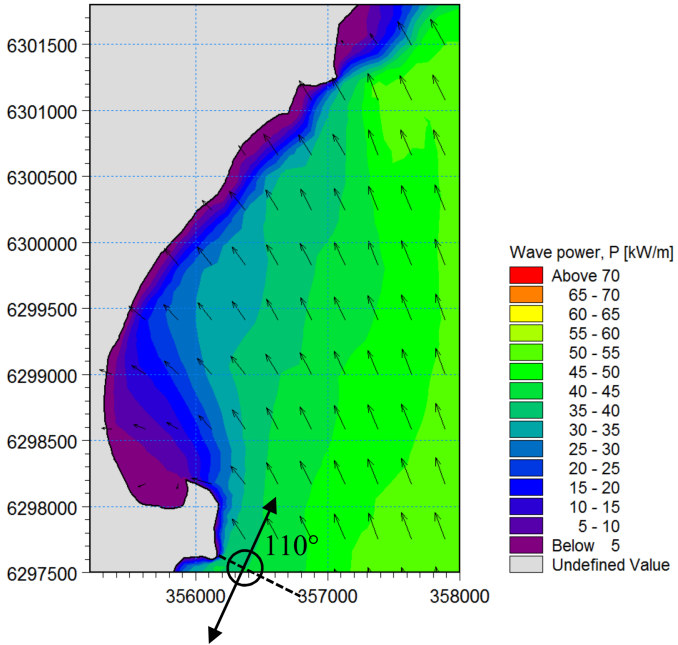

ETL (116°, 23%)

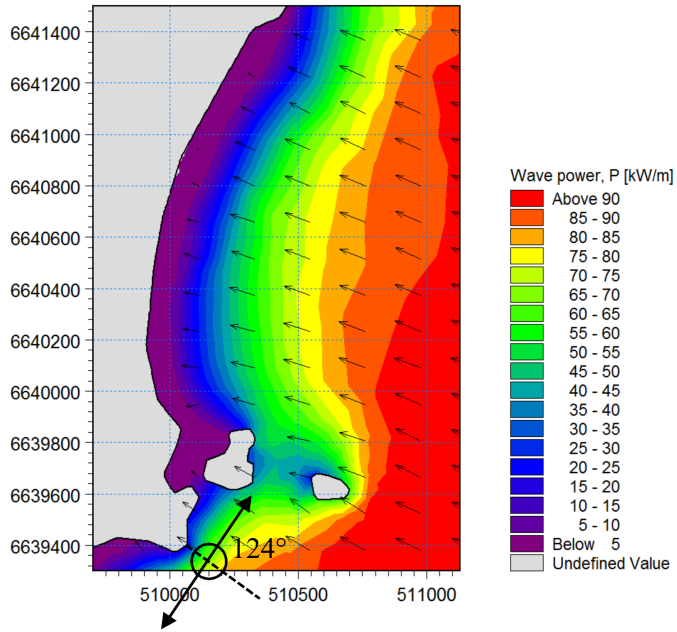

ITL (142°, 25%)

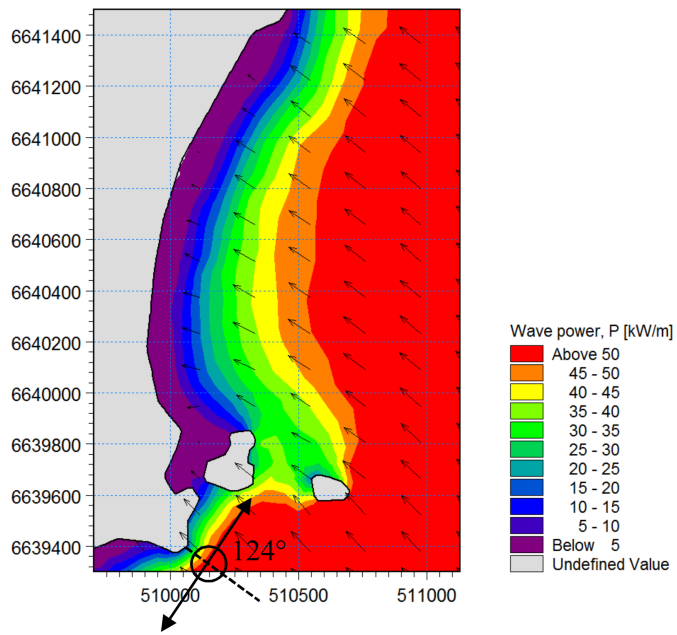

SSL (149°, 21%)

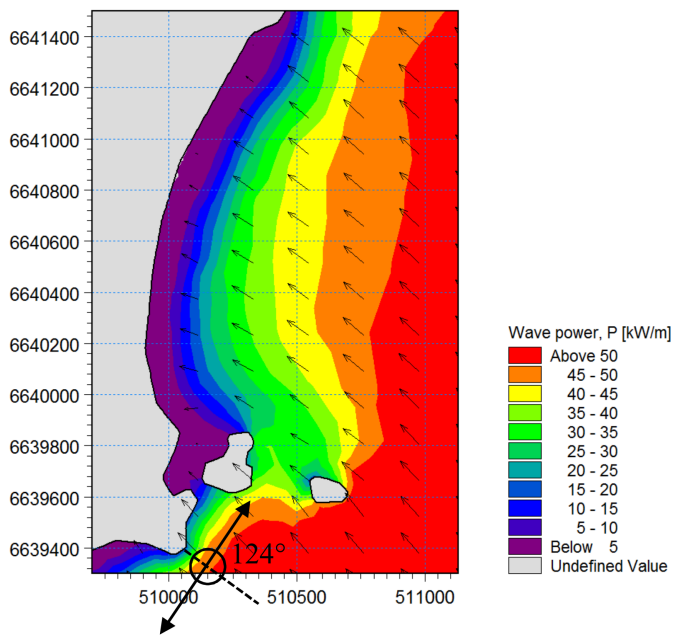

STL (161°, 14%)

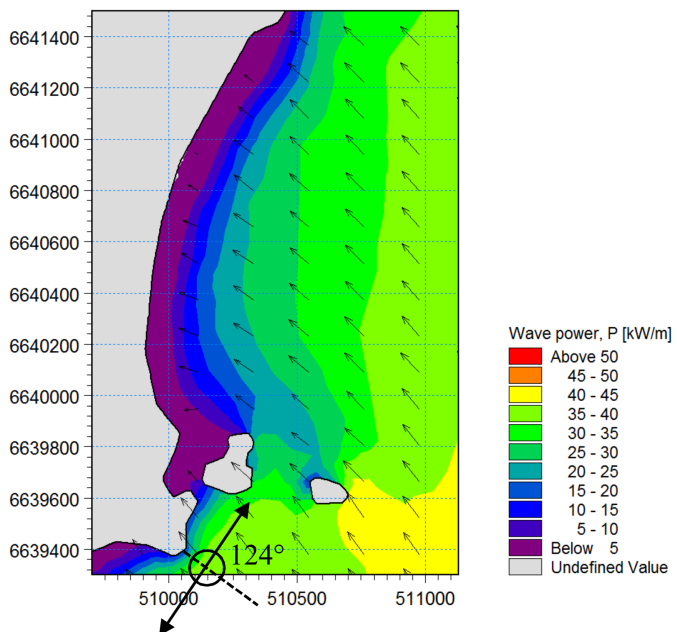

Byron Bay (North Coast NSW)

ETL (115°, 12%)

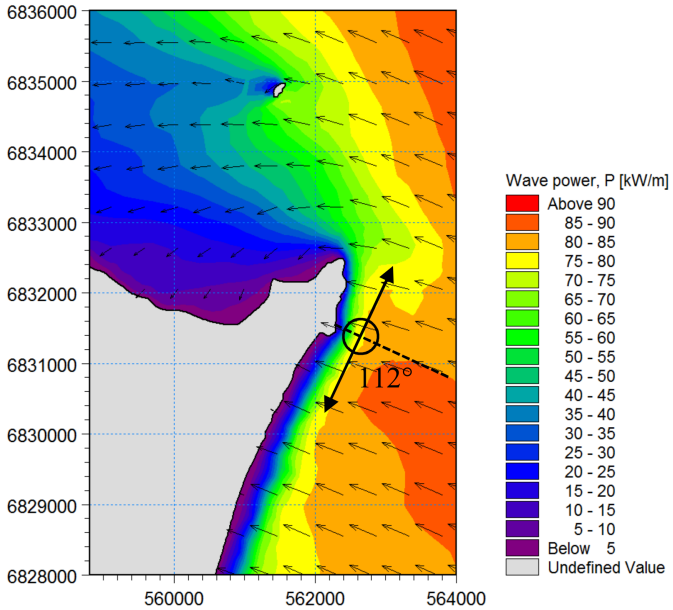

AI (139°, 23%)

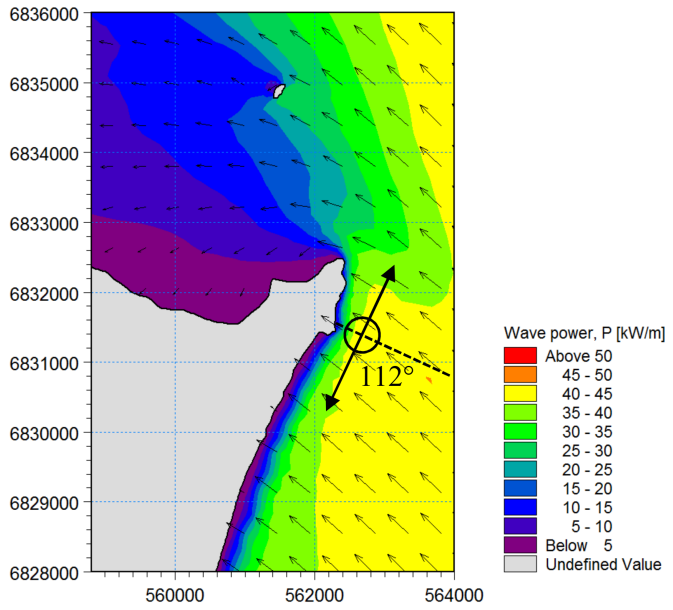

ITL (156°, 15%)

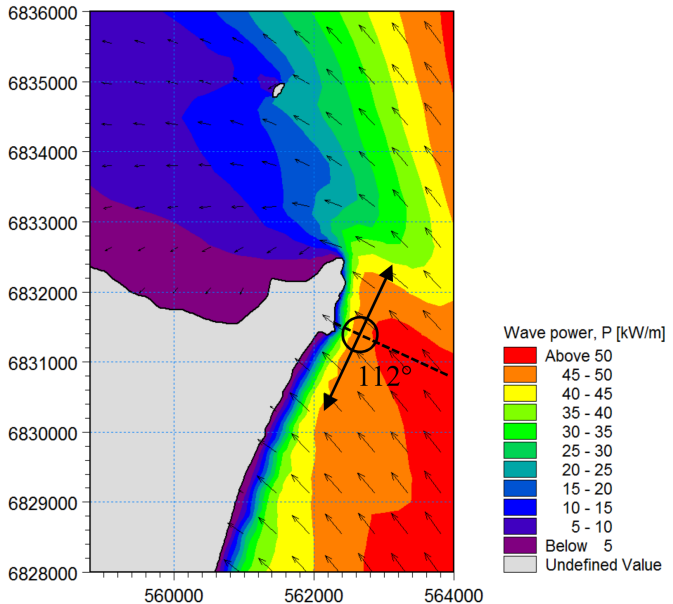

SSL (167°, 26%)

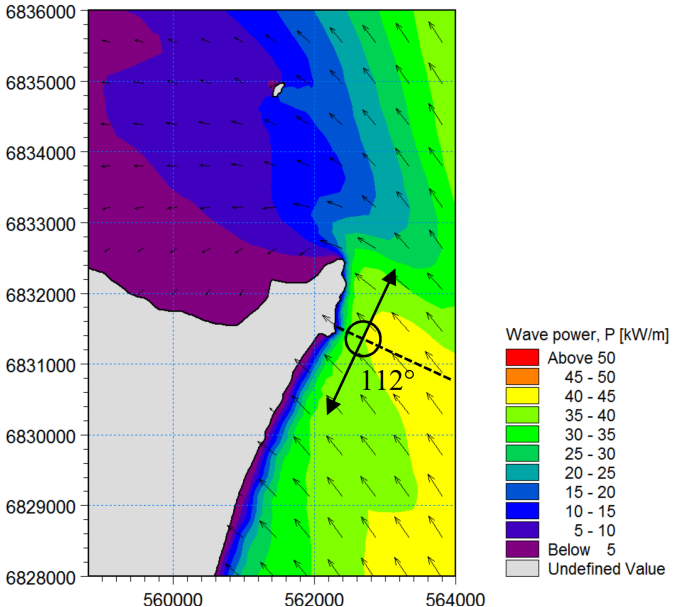

A. Storm Wave Propagation

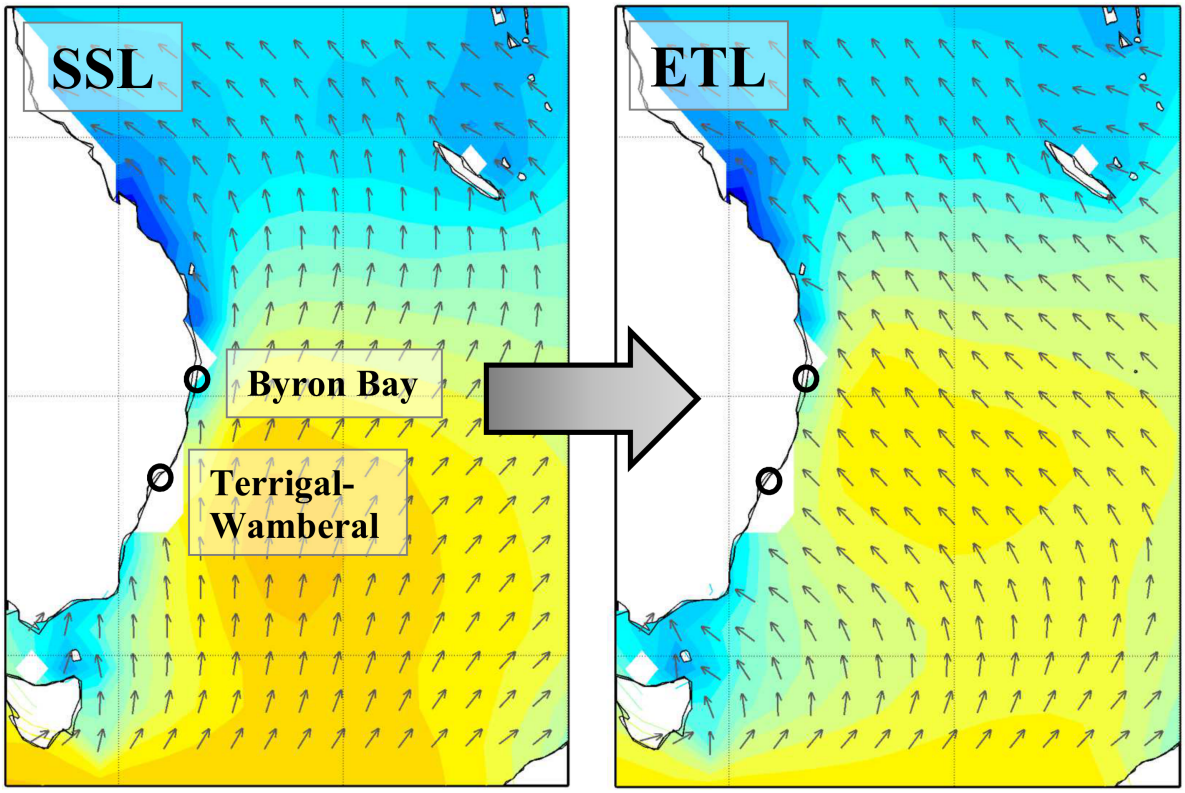

B. Nearshore Wave Power

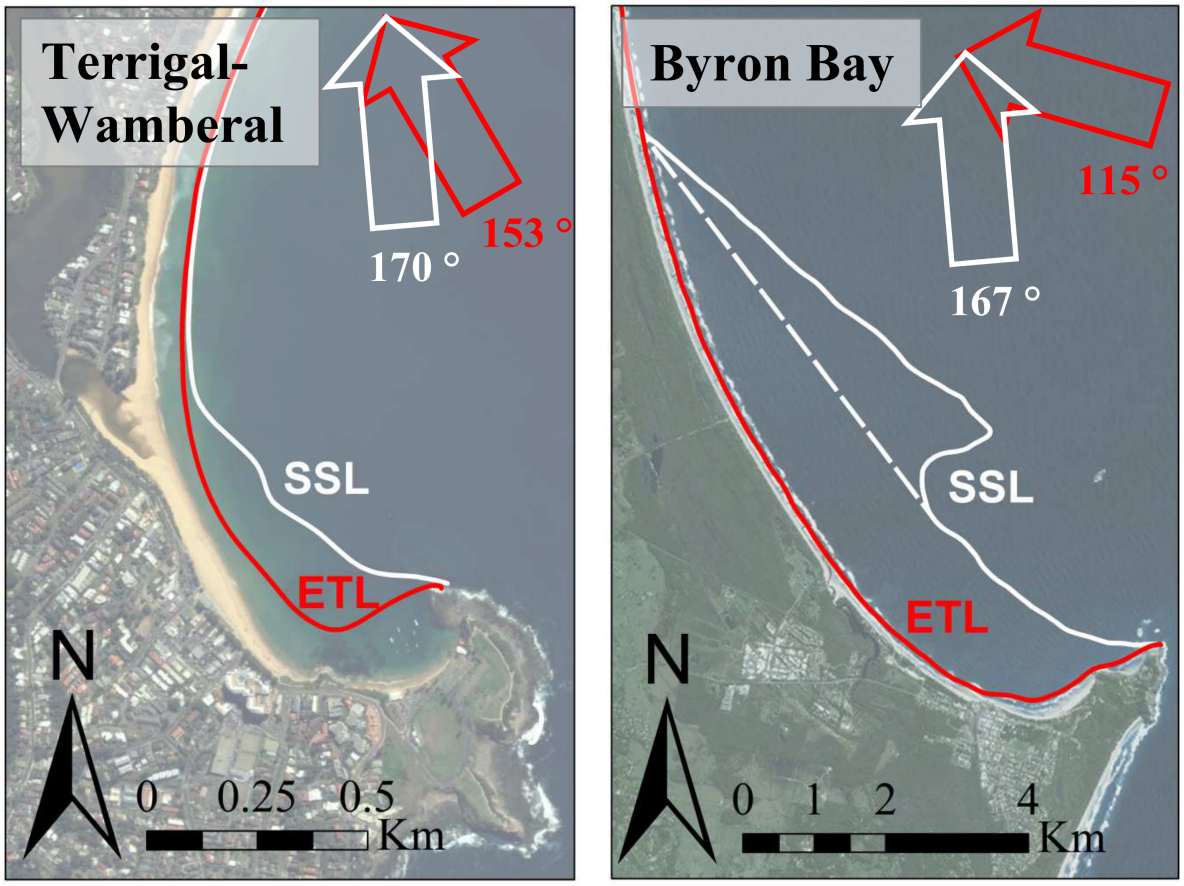

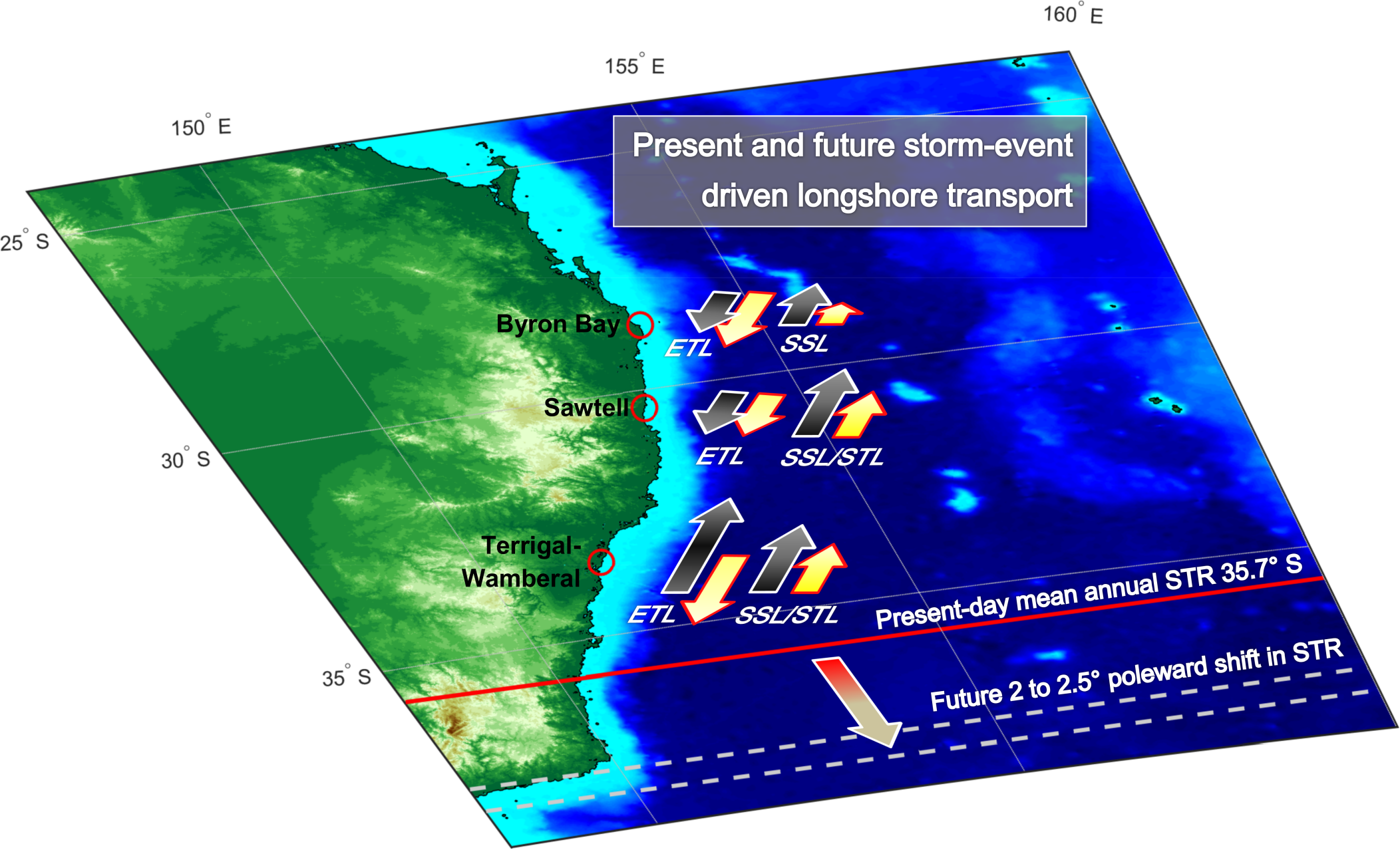
160° E
155° E
150° E
25° S
30° S
35° S
Present and future storm-event driven longshore transport
Byron Bay
Sawtell
Terrigal-Wamberal
ETL
SSL
ETL
SSL/STL
ETL
SSL/STL
Present-day mean annual STR 35.7° S
Future 2 to 2.5° poleward shift in STR